

# Gemcitabine and cisplatin plus nivolumab as organ-sparing treatment for muscle-invasive bladder cancer: a phase 2 trial

Received: 10 January 2023

Accepted: 24 August 2023

Published online: 2 October 2023

 Check for updates

A list of authors and their affiliations appears at the end of the paper

Cystectomy is a standard treatment for muscle-invasive bladder cancer (MIBC), but it is life-altering. We initiated a phase 2 study in which patients with MIBC received four cycles of gemcitabine, cisplatin, plus nivolumab followed by clinical restaging. Patients achieving a clinical complete response (cCR) could proceed without cystectomy. The co-primary objectives were to assess the cCR rate and the positive predictive value of cCR for a composite outcome: 2-year metastasis-free survival in patients forgoing immediate cystectomy or  $\leq$ ypT1N0 in patients electing immediate cystectomy. Seventy-six patients were enrolled; of these, 33 achieved a cCR (43%, 95% confidence interval (CI): 32%, 55%), and 32 of 33 who achieved a cCR opted to forgo immediate cystectomy. The positive predictive value of cCR was 0.97 (95% CI: 0.91, 1), meeting the co-primary objective. The most common adverse events were fatigue, anemia, neutropenia and nausea. Somatic alterations in pre-specified genes (*ATM*, *RBI*, *FANCC* and *ERCC2*) or increased tumor mutational burden did not improve the positive predictive value of cCR. Exploratory analyses of peripheral blood mass cytometry and soluble protein analytes demonstrated an association between the baseline and on-treatment immune contexture with clinical outcomes. Stringently defined cCR after gemcitabine, cisplatin, plus nivolumab facilitated bladder sparing and warrants further study. ClinicalTrials.gov identifier: [NCT03451331](https://clinicaltrials.gov/ct2/show/study/NCT03451331).

Radical cystectomy is a standard treatment for muscle-invasive bladder cancer (MIBC). However, radical cystectomy is a life-changing operation due to the need for urinary diversion and is associated with a 90-d mortality risk of up to 6–8% (ref. 1). Neoadjuvant cisplatin-based chemotherapy before radical cystectomy confers improved survival in patients with MIBC<sup>2,3</sup>. Although the intent of neoadjuvant chemotherapy is eradication of micrometastatic disease, neoadjuvant cisplatin-based chemotherapy after transurethral resection of bladder tumor (TURBT) yields a pathological complete response (pCR) at the time of cystectomy in approximately 30% of

patients<sup>2,4</sup>. Paradoxically, a pCR can be determined only after the bladder has been surgically removed.

Given the potential to achieve a pCR with TURBT followed by neoadjuvant chemotherapy, the need for cystectomy to achieve cure in all patients has been questioned. Early single-center retrospective studies reported that long-term bladder-intact disease-free survival is achievable in a select subset of patients with MIBC treated with TURBT plus systemic therapy, and contemporary retrospective series have substantiated such results<sup>5–7</sup>. However, challenges to the broader application of this treatment paradigm have included

✉ e-mail: [matthew.galsky@mssm.edu](mailto:matthew.galsky@mssm.edu)

(1) a paucity of prospective studies<sup>8,9</sup>; (2) a lack of rigorous and standardized approaches to both measure (that is, clinical restaging) and define clinical complete response (cCR); (3) poor understanding of the impact of later cystectomy on cancer control in patients with a cCR who develop local recurrence after a period of initial surveillance; and (4) suboptimal systemic therapeutic regimens.

Single-agent PD-1/PD-L1 immune checkpoint blockade followed by cystectomy for the treatment of MIBC has been shown to yield a pCR in 30–40% of patients<sup>10,11</sup>. Cisplatin may induce favorable immunomodulatory effects<sup>12</sup>, providing rationale for regimens combining neoadjuvant chemotherapy plus PD-1/PD-L1 blockade. In phase 2 studies, neoadjuvant gemcitabine, cisplatin, plus PD-1/PD-L1 blockade has demonstrated pCR rates of 40–50%, leading to the initiation of several phase 3 trials (NCT03661320, NCT03732677 and NCT03924856)<sup>13,14</sup>.

The integration of molecular biomarkers may further improve selection of patients with MIBC who could be treated definitively with TURBT plus systemic therapy. Somatic alterations in genes encoding proteins involved in DNA damage repair (DDR) in pre-treatment TURBT tissue have been correlated with a higher pCR rate with cisplatin-based neoadjuvant chemotherapy<sup>15–20</sup>. DDR gene alterations have also been associated with an increased likelihood of response to PD-1/PD-L1 blockade, potentially mediated by increased tumor mutational burden (TMB), raising the hypothesis that such tumors may be particularly sensitive to cisplatin plus PD-1/PD-L1 blockade combination regimens<sup>21,22</sup>.

To further evaluate the role of TURBT plus systemic therapy as definitive treatment for MIBC, we designed a phase 2 trial integrating (1) cisplatin-based chemotherapy plus PD-1 blockade; (2) standardized clinical restaging; and (3) translational analyses seeking to explore genomic, radiologic and immunologic biomarkers to refine future patient selection for this approach. Our primary goal was to test whether uniformly assessed and consistently defined cCR could identify patients who could safely forgo immediate cystectomy. We reasoned that a potentially effective personalized risk-adapted strategy would (1) tolerate missing some patients who might have been suitable candidates to forgo immediate cystectomy in favor of maximizing identification of patients who fare well without immediate cystectomy and (2) incorporate the ability of later cystectomy to achieve favorable cancer-related outcomes in the subset of patients with a cCR who experience local recurrence after initial surveillance. Therefore, our primary objectives were to estimate the cCR rate and to assess the positive predictive value of cCR for a composite outcome measure (2-year metastasis-free survival in patients forgoing immediate cystectomy or <ypT1N0 in patients electing immediate cystectomy; Extended Data Fig. 1).

## Results

### Patient characteristics and treatment

Cisplatin-eligible patients with cT2–T4aN0M0 MIBC received treatment with four cycles of gemcitabine and cisplatin plus nivolumab (Extended Data Fig. 1) followed by clinical restaging. Clinical restaging comprised magnetic resonance imaging (MRI) of the abdomen and pelvis (unless contraindicated, in which case computed tomography (CT) scans were substituted), CT of the chest, cystoscopy with biopsies according to a recommended template (Methods) and urine cytology. A cCR was defined as (1) no evidence of high-grade malignancy on biopsy; (2) no malignant cells on urine cytology; and (3) no definitive evidence of local or metastatic disease on cross-sectional imaging. Patients achieving a cCR were offered the option to proceed with cystectomy versus retain their bladder and receive eight additional doses of nivolumab (administered every 2 weeks) followed by surveillance. Patients not achieving a cCR were recommended to proceed with cystectomy.

Between 8 August 2018 and 24 November 2020, 76 patients were enrolled with baseline characteristics as detailed in Table 1. The disposition of patients on study is outlined in Fig. 1a. Among the 76 patients enrolled, 72 underwent clinical restaging; one patient did not undergo

**Table 1 | Baseline patient characteristics (n=76)**

Characteristic	Category	n	% or range
Sex	Female	16	21%
	Male	60	79%
Race	Caucasian	58	76%
	African American	1	1%
	Asian	9	12%
	Unknown	8	11%
Age (years)	Median	69	39–85
Clinical stage	cT2N0M0	43	57%
	cT3N0M0	24	32%
	cT4N0M0	9	12%
Histology	UC	57	75%
	UC with squamous	7	9%
	UC with glandular	2	3%
	UC with micropapillary	6	8%
	UC with other variant	4	5%

restaging due to the development of metastatic disease, and three patients developed adverse events (cerebrovascular accident, deep venous thrombosis and increase in creatinine) and proceeded with cystectomy.

### Copriary endpoint analysis

The co-primary endpoint of cCR was achieved in 33 of 76 patients (43%, 95% confidence interval (CI): 32%, 55%; Fig. 1a). Lower baseline clinical T stage was associated with a higher likelihood of a cCR, although cCRs were observed in patients with cT2–T4 disease (Extended Data Table 1). Among the 33 patients achieving a cCR, only one opted for immediate cystectomy with surgical pathology, revealing a low-grade ypTaNO urothelial cancer (UC). As shown in Fig. 1b, the positive predictive value of cCR (co-primary endpoint) for the composite outcome measure was 0.97 (95% CI: 0.91, 1), with the lower bound of the 95% CI exceeding the pre-specified threshold of 80%.

The median metastasis-free and overall survival for the entire study cohort was not reached at the time of the data lock (secondary endpoints). To further contextualize the prognostic impact of achieving a cCR as related to metastasis-free survival and overall survival, a post hoc landmark analysis was performed using the time of clinical restaging as ‘time 0’. On landmark analysis from the time of restaging, patients achieving a cCR experienced significantly longer metastasis-free survival and overall survival compared to patients not achieving a cCR (Fig. 1c,d).

### Clinical outcomes according to cCR status

The median follow-up for patients achieving a cCR was 30 months (range, 18–42 months) at the data lock and the clinical outcomes of this group are detailed in Fig. 2. Thirty-two patients opting to forgo immediate cystectomy received a median of eight (range, 0–8) cycles of maintenance nivolumab, and eight of 32 patients later underwent cystectomy for local recurrence (including one patient for an abnormal MRI scan with no cancer detected on TURBT or cystectomy). The clinical stage at the time of recurrence and the pathological stage at cystectomy are summarized in Supplementary Table 1; seven of eight patients had ≤ypT2N0 disease on cystectomy. Two additional patients developed non-invasive local recurrence during follow-up (low-grade cTa and cTis) and were managed with TURBT and intravesical BCG, respectively, without evidence of subsequent recurrence. Two of the 32 patients developed metastatic disease, including one patient with

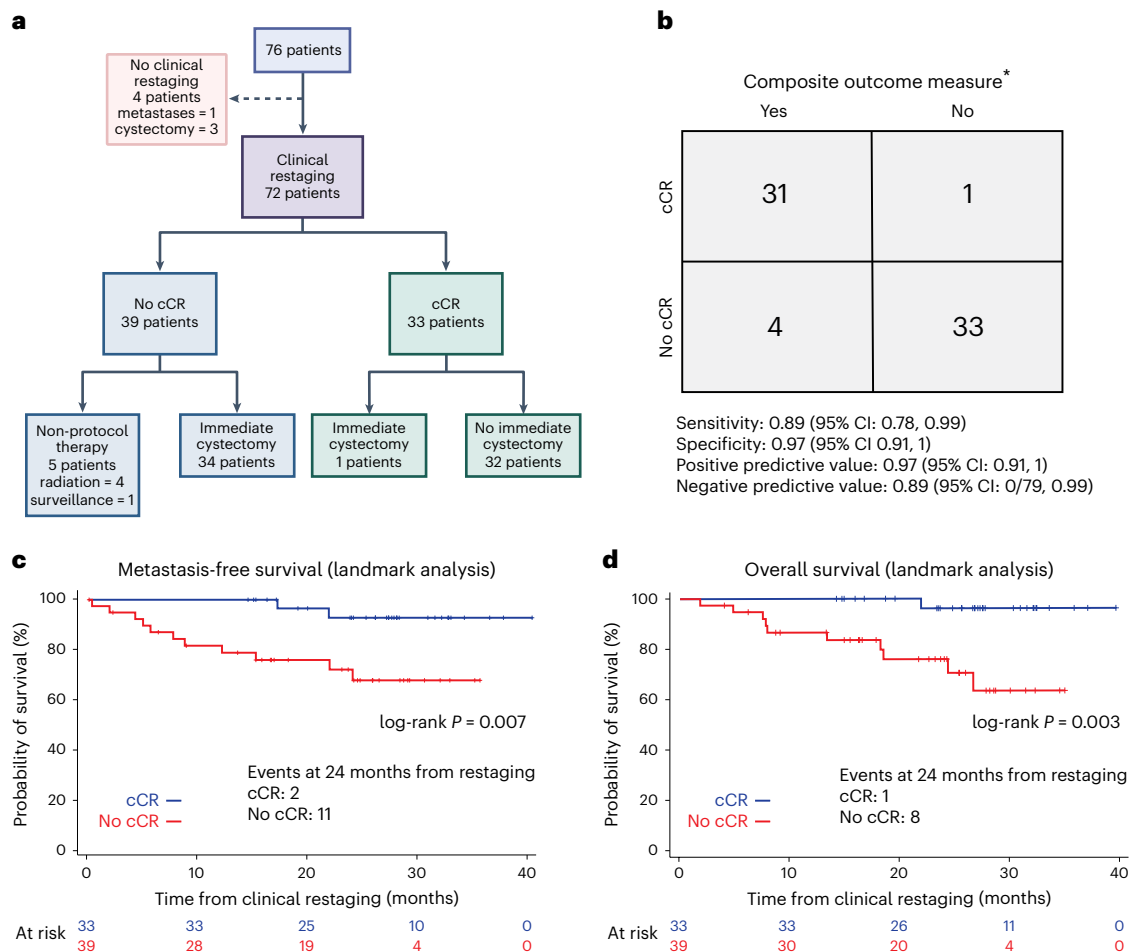


**Fig. 1 | Study design and primary objectives of HCRN GU16-257.** **a**, CONSORT diagram outlining disposition of patients enrolled on HCRN GU16-257 and demonstrating co-primary objective of estimating the cCR rate. **b**, Contingency table informing co-primary objective of assessing the positive predictive value of cCR for the composite outcome measure of 2-year metastasis-free survival in patients forgoing immediate cystectomy or <ypT1N0 in patients undergoing immediate cystectomy ( $n = 69$  of 76 total patients). Seven patients were excluded for the following reasons: four patients who did not undergo clinical response assessment; two patients who did not achieve a cCR, who did not pursue cystectomy and who were lost to follow-up before 2 years; and one patient who achieved a cCR and without evidence of local or distant recurrence at 18 months

and who was subsequently lost to follow-up. **c**, Metastasis-free survival according to cCR versus no cCR using landmark timepoint of post-cycle 4 restaging ( $n = 72$ ; four patients were excluded who did not undergo clinical response assessment). Estimating metastasis-free survival was a secondary objective of the study. **d**, Overall survival according to cCR versus no cCR using landmark timepoint of post-cycle 4 restaging ( $n = 72$ ; four patients were excluded who did not undergo clinical response assessment). Estimating overall survival was a secondary objective of the study. **a** and **b** were created with BioRender. \*Composite outcome measure: 2-year metastasis-free survival in patients forgoing immediate cystectomy or <ypT1N0 in patients undergoing immediate cystectomy.

metastatic disease diagnosed 10 months after a cystectomy revealed ypT4N1 disease and the other presenting with malignant ascites with no evidence of recurrence in the bladder.

Thirty-nine patients did not achieve a cCR, and 34 of 39 underwent cystectomy (four received off protocol radiation and one declined any local therapy). The relationship between clinical restaging results in patients not achieving a cCR and the final cystectomy pathological stage is summarized in Supplementary Table 2.

### Safety

The treatment-emergent adverse events are detailed in Extended Data Table 2 and Supplementary Table 4. Grade  $\geq 3$  treatment-emergent adverse events occurred in 75% of patients. The most common all-grade treatment-emergent adverse events were fatigue, anemia, neutropenia and nausea, and the most common grade  $\geq 3$  treatment-emergent adverse events were anemia, neutropenia and urinary tract infections. One patient died due to sepsis subsequent to a bowel perforation occurring at the time of cystectomy, which was not attributed to systemic therapy.

### Genomic features associated with clinical outcomes

In an effort to refine future selection of patients for this risk-adapted treatment approach, a secondary objective of the study was to assess whether the presence of a set of genomic alterations in baseline TURBT tissue would enhance the positive predictive value of cCR. Tumor-only targeted DNA sequencing of pre-treatment TURBT tissue was available from 73 of 76 patients (Fig. 3). A panel of genes that, when mutated, had previously been correlated with response to cisplatin-based chemotherapy or PD-1/PD-L1 blockade (*ERCC2*, *RBI*, *ATM* and *FANCC*)<sup>15–22</sup>, as well as increased TMB (using an established cutpoint of  $\geq 10$  mutations per megabase (mut/Mb), which has served as the basis for tumor-agnostic PD-1 blockade regulatory approvals and for which sensitivity and specificity in bladder cancer has been established<sup>23,24</sup>), was pre-specified for analysis. Similar to the co-primary objective, the intent of this secondary objective was to assess the positive predictive value of the genomic alterations, added to cCR, for the composite outcome measure of 2-year metastasis-free survival in patients forgoing immediate cystectomy or <ypT1N0 in patients undergoing immediate cystectomy. However, the high positive predictive value of cCR alone precluded this analysis,

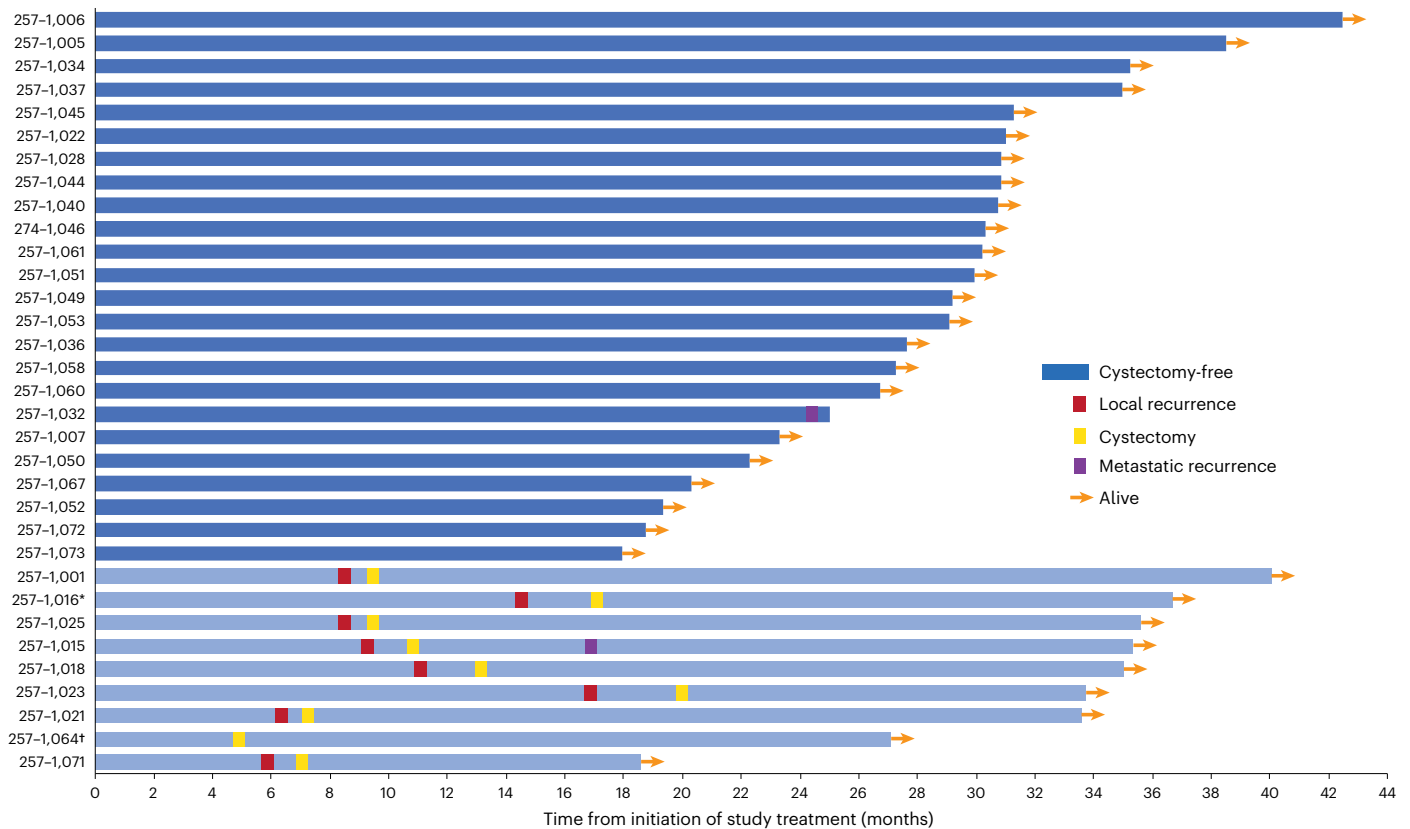


**Fig. 2 | Clinical outcomes of patients enrolled on HCRN GU16-257 achieving a cCR.** \* Patient underwent cystectomy for radiographic changes concerning for local recurrence without evidence of cancer on biopsy or final cystectomy specimen. † Patient opted for immediate cystectomy.

and, instead, the positive predictive value of cCR with or without the pre-specified genomic alterations for the composite outcome of 2-year bladder-intact survival in patients forgoing immediate cystectomy or  $\leq$ ypT1N0 in patients undergoing immediate cystectomy was explored. As shown in Table 2 (and associated contingency table, Supplementary Table 4), the positive predictive value of the pre-specified genomic alterations added to cCR status did not clearly enhance the positive predictive value of cCR alone. The possible exception was the presence of a pathogenic mutation in *FANCC*, *ATM* and/or *RBI* in patients with a cCR, which was limited to five patients, all of whom had pathogenic *RBI* mutations; the relevance of this finding is unclear.

An exploratory analysis was also performed to assess the association between the pre-specified genomic alterations and achieving a cCR. cCR rates were higher in patients with tumors harboring *ERCC2* mutations or TMB  $\geq$ 10 mut/Mb versus patients with tumors without such alterations, but these associations did not achieve statistical significance after correction for false discovery (Extended Data Table 3).

### Radiographic features associated with clinical outcomes

Conventional radiographic assessments are largely qualitative, and bladder tumors are particularly difficult to assess given the anatomy of the bladder and challenges distinguishing post-treatment bladder wall thickening from residual tumor<sup>25</sup>. Post-cycle-4 restaging MRI scans were recommended per protocol (unless otherwise contraindicated or not feasible, in which case CT scans were substituted) and were obtained in 50 of 76 patients. An exploratory analysis was performed involving central review of the MRI images with assignment of Vesical Imaging-Reporting and Data System (VI-RADS) scores<sup>25</sup> (Extended Data Fig. 2a,b) by two independent reviewers blinded to clinical outcomes (weighted kappa: 0.63; 95% CI: 0.44, 0.82). The distribution of VI-RADS scores at the time of restaging, according to cCR status, is shown in Extended Data Fig. 2c. Only two patients who achieved a cCR had a

restaging VI-RADS score greater than 2, although both experienced a subsequent local recurrence. Although VI-RADS scores of 1–2 versus 3–5 were enriched in patients achieving a cCR, 44% of patients not achieving a cCR had restaging VI-RADS scores of 1–2 (Extended Data Fig. 2c). On landmark analysis from the time of restaging, restaging VI-RADS score of  $\leq$ 2 versus  $>$ 2 was associated with significantly longer metastasis-free survival ( $P = 0.0002$  from log-rank test; Extended Data Fig. 2d).

### Immunological features associated with clinical outcomes

To determine whether baseline and/or on-treatment immune parameters were associated with achieving a cCR or with metastasis-free survival or overall survival, additional exploratory analyses were pursued. PD-L1 immunohistochemical staining (22C3 antibody clone) of baseline TURBT specimens was completed in a central laboratory. A higher PD-L1 combined positive score was associated with a higher cCR rate, although the relationship between higher PD-L1 expression and longer metastasis-free survival or overall survival did not achieve statistical significance (Extended Data Fig. 3a–c). Mass cytometry (CyTOF) was performed on peripheral blood mononuclear cells (PBMCs) to define frequency of immune subsets, and a panel of 92 soluble protein analytes was measured in the plasma (Olink) on cycle 1, day 1 and cycle 3, day 1 (Fig. 4a). Protein analytes were also measured in the urine at the time of post-cycle-4 clinical restaging. Although the abundance of specific immune cell populations on cycle 1, day 1 and cycle 3, day 1 correlated with achieving a cCR versus not, such findings did not achieve statistical significance after correction for false discovery (Extended Data Fig. 4a). A higher abundance of cycle 1, day 1 naive CD4<sup>+</sup> T cells in peripheral blood was associated with significantly longer metastasis-free survival and overall survival (Fig. 4b,c and Extended Data Fig. 4b). On landmark analysis, a higher abundance of circulating naive CD8 T cells on cycle 3, day 1 was associated with significantly longer metastasis-free survival and overall survival (Fig. 4d,e and Extended Data Fig. 4c).

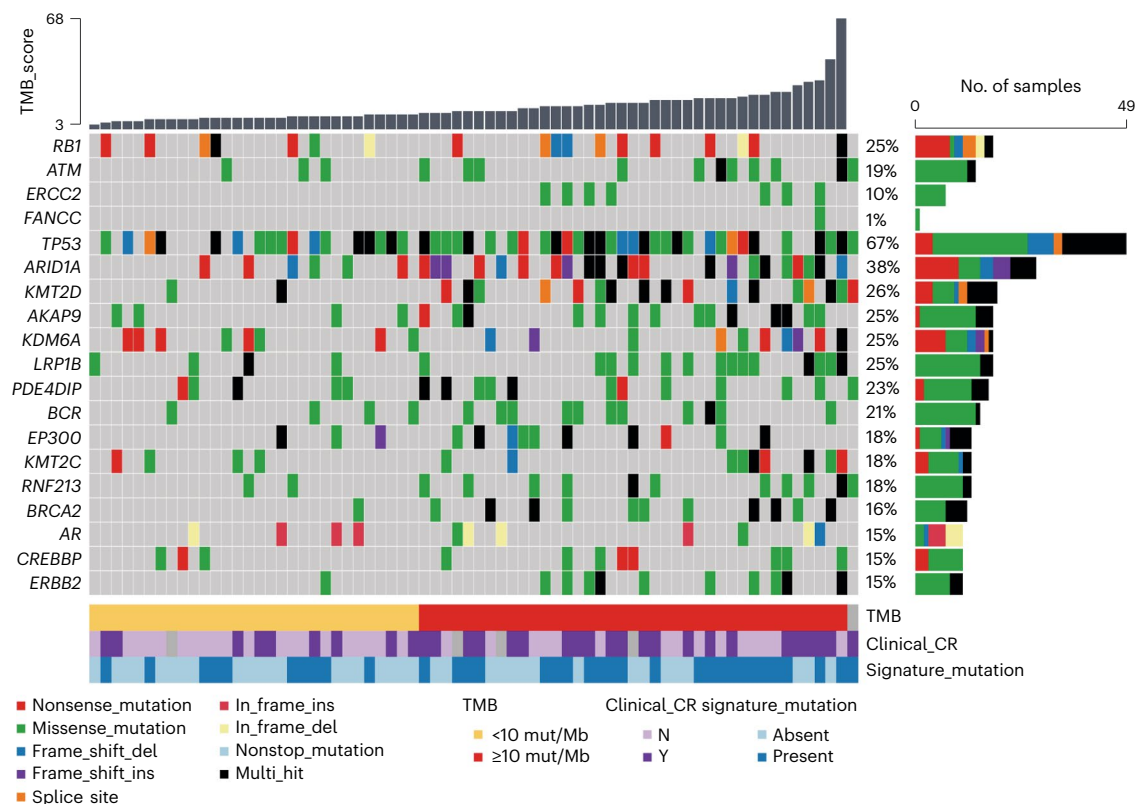


**Fig. 3 | Genomic alterations in pre-treatment tumor tissue and association with clinical outcomes.** Oncoplot revealing frequently mutated genes based on DNA sequencing of pre-treatment transurethral resection of bladder tumor specimens among 73 patients. Oncoplot is arranged according to TMB (Methods)

and annotated based on the presence or absence of a mutation in a pre-specified set of genes (*RB1*, *ATM*, *ERCC2* and *FANCC*), referred to as ‘Signature\_mutations’ and according to cCR categorization. Mutations are annotated: del, deletion; ins, insertion.

Several plasma protein analytes significantly increased on treatment from cycle 1, day 1 to cycle 3, day 1 (Extended Data Fig. 5a). Cycle 1, day 1 levels of plasma analytes were not significantly associated with cCR after correction for false discovery (Fig. 4f). However, cycle 3, day 1 plasma levels of TNF-related apoptosis-inducing ligand (TRAIL), FasL and CD244 were significantly higher in patients achieving a cCR versus not (Fig. 4g,h). Higher cycle 1, day 1 plasma levels of several analytes were associated with significantly shorter metastasis-free and overall survival, including IL6 and angiopoietin-2 (ANGPT2) (Fig. 4i,j and Extended Data Fig. 5b,c). On landmark analysis at cycle 3, day 1, similar associations with metastasis-free survival and overall survival were observed for several plasma analytes, such as IL6 and ANGPT2, based on either cycle 3, day 1 levels or on-treatment changes in levels from cycle 1, day 1 to cycle 3, day 1 (Fig. 4k,l and Extended Data Fig. 5d–h). No urine analytes from samples obtained at the time of clinical restaging were significantly associated with achieving a cCR after correction for false discovery (Extended Data Fig. 6a), whereas increased urine levels of analytes, such as epidermal growth factor (EGF), at the clinical restaging timepoint were associated with both significantly inferior metastasis-free survival and overall survival (Fig. 4m and Extended Data Fig. 6b).

## Discussion

To our knowledge, this is among the first prospective trials to test TURBT plus cisplatin-based chemotherapy as definitive bladder-sparing treatment for MIBC; the first to define the performance characteristics of uniformly assessed and defined cCR as a tool for patient selection for this strategy; and the first to integrate immune checkpoint blockade into this approach. Our study demonstrates that stringently defined cCR is associated with favorable survival outcomes and that prolonged

bladder-intact survival is achievable in a large subset of patients with MIBC and a cCR to TURBT and gemcitabine, cisplatin, plus nivolumab.

Radical cystectomy or radiation therapy are mainstays of local treatment for MIBC. However, despite such treatments, more than 50% of patients experience metastatic recurrence<sup>2,26</sup>. Radical cystectomy requires urinary diversion and is associated with a non-negligible risk of morbidity and mortality<sup>1</sup>. Concurrent chemoradiation is associated with an approximately 17% risk of late grade  $\geq 2$  pelvic toxicity, and approximately one-third of patients report worsening quality of life 6 months after completing treatment and persisting on long-term follow-up<sup>27,28</sup>. Furthermore, salvage cystectomy due to local recurrence is required in 12–19% of patients treated with radiation with or without concurrent chemotherapy<sup>29</sup>. Systemic therapy is associated with a different constellation of potential adverse events, and gemcitabine, cisplatin, plus PD-1 blockade demonstrated a toxicity profile consistent with other studies<sup>13,14</sup>. Each of these treatment modalities is an important component of optimal treatment of MIBC, and each is associated with specific tradeoffs. Risk-adapted MIBC treatment paradigms that balance both efficacy and survivorship while also reducing treatment-related burden could represent an important addition to patient-centered care.

Although the IMvigor 130 and Keynote 361 studies exploring concurrent administration of platinum-based chemotherapy and PD-1/PD-L1 blockade in patients with metastatic bladder cancer did not demonstrate improvements in survival, those studies pooled patients treated with cisplatin-based and carboplatin-based chemotherapy<sup>30,31</sup>. Cisplatin may induce distinct immunomodulatory effects and combine more favorably with immune checkpoint blockade<sup>32</sup>. Consistent with this hypothesis, CheckMate 901, exploring gemcitabine, cisplatin, plus nivolumab versus gemcitabine plus cisplatin in patients

**Table 2 | Performance characteristics of cCR with or without genomic alterations in baseline TURBT tissue for a composite outcome measure of 2-year bladder-intact survival in patients forgoing immediate cystectomy or <ypT1NO in patients undergoing immediate cystectomy**

Measure	Performance metric
<b>cCR</b>	
Sensitivity	0.85 (95% CI: 0.72, 1.00)
Specificity	0.79 (95% CI: 0.66, 0.91)
Positive predictive value	0.72 (95% CI: 0.56, 0.87)
Negative predictive value	0.89 (95% CI: 0.79, 0.99)
<b>cCR + any mutation in <i>FANCC</i>, <i>ATM</i> and/or <i>RB1</i></b>	
Sensitivity	0.31 (95% CI: 0.13, 0.49)
Specificity	0.93 (95% CI: 0.84, 1.00)
Positive predictive value	0.73 (95% CI: 0.46, 0.99)
Negative predictive value	0.67 (95% CI: 0.55, 0.80)
<b>cCR + any pathogenic<sup>a</sup> mutation in <i>FANCC</i>, <i>ATM</i> and/or <i>RB1</i></b>	
Sensitivity	0.19 (95% CI: 0.04, 0.34)
Specificity	1.00 (95% CI: 1.00, 1.00)
Positive predictive value	1.00 (95% CI: 1.00, 1.00)
Negative predictive value	0.66 (95% CI: 0.54, 0.78)
<b>cCR + any mutation in <i>ERCC2</i></b>	
Sensitivity	0.12 (95% CI: 0.00, 0.24)
Specificity	0.95 (95% CI: 0.88, 1.00)
Positive predictive value	0.60 (95% CI: 0.17, 1.00)
Negative predictive value	0.62 (95% CI: 0.50, 0.74)
<b>cCR + any pathogenic<sup>a</sup> mutation <i>ERCC2</i></b>	
Sensitivity	0.08 (95% CI: 0.00, 0.18)
Specificity	0.95 (95% CI: 0.88, 1.00)
Positive predictive value	0.50 (95% CI: 0.01, 0.99)
Negative predictive value	0.61 (95% CI: 0.49, 0.73)
<b>cCR + any mutation in <i>FANCC</i>, <i>ATM</i>, <i>RB1</i> and/or <i>ERCC2</i></b>	
Sensitivity	0.38 (95% CI: 0.20, 0.57)
Specificity	0.90 (95% CI: 0.81, 0.99)
Positive predictive value	0.71 (95% CI: 0.48, 0.95)
Negative predictive value	0.69 (95% CI: 0.57, 0.82)
<b>cCR + any pathogenic<sup>a</sup> mutation in <i>FANCC</i>, <i>ATM</i>, <i>RB1</i> and/or <i>ERCC2</i></b>	
Sensitivity	0.23 (95% CI: 0.07, 0.39)
Specificity	0.95 (95% CI: 0.88, 1.00)
Positive predictive value	0.75 (95% CI: 0.45, 1.00)
Negative predictive value	0.66 (95% CI: 0.53, 0.78)
<b>cCR + TMB <math>\geq</math>10 mut/Mb</b>	
Sensitivity	0.63 (95% CI: 0.43, 0.82)
Specificity	0.85 (95% CI: 0.74, 0.96)
Positive predictive value	0.71 (95% CI: 0.52, 0.91)
Negative predictive value	0.79 (95% CI: 0.67, 0.91)
<b>cCR + any <i>FANCC</i>, <i>ATM</i>, <i>RB1</i>, <i>ERCC2</i>, and/or TMB <math>\geq</math> 10 mut/Mb</b>	
Sensitivity	0.61 (95% CI: 0.43, 0.80)
Specificity	0.85 (95% CI: 0.74, 0.96)
Positive predictive value	0.73 (95% CI: 0.54, 0.91)
Negative predictive value	0.77 (95% CI: 0.65, 0.90)

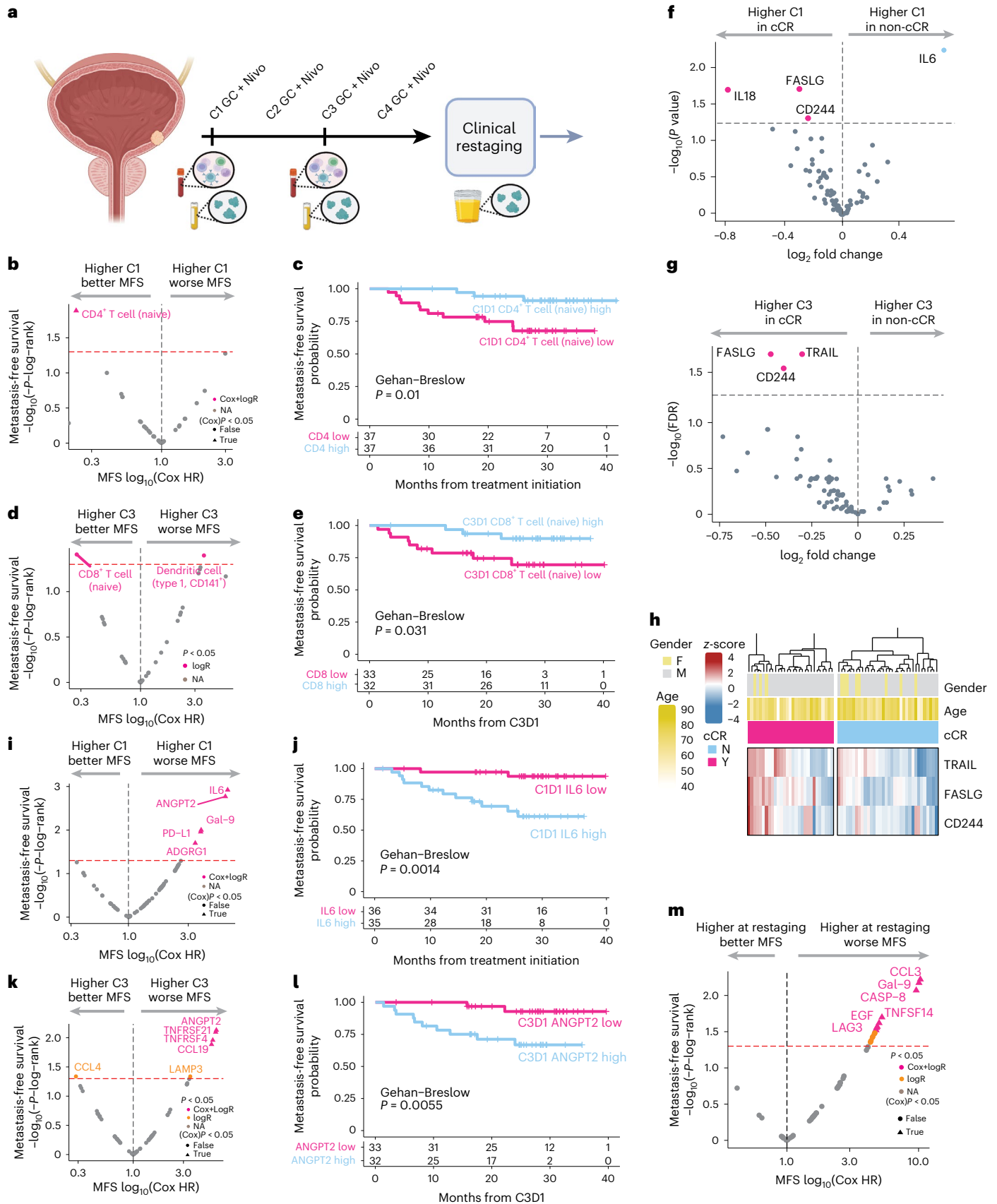
<sup>a</sup>At least presumed pathogenic mutation, as defined in the Methods.

with metastatic bladder cancer, did demonstrate an improvement in progression-free and overall survival with the immunotherapy combination (<https://news.bms.com/news/corporate-financial/2023/Opdivo-nivolumab-in-Combination-with-Cisplatin-Based-Chemotherapy-Shows-Overall-Survival-and-Progression-Free-Survival-Benefit-for-Cisplatin-Eligible-Patients-with-Unresectable-or-Metastatic-Urothelial-Carcinoma-in-the-Phase-3-CheckMate-901-Trial/default.aspx>). Sequential chemotherapy followed by switch maintenance immune checkpoint blockade has also demonstrated improved progression-free and overall survival in metastatic bladder cancer and has become a standard of care<sup>33,34</sup>. The contribution of concurrent versus sequential nivolumab to the favorable outcomes observed in our study cannot be fully delineated.

Our study has potential limitations. The median follow-up of patients achieving a cCR was 30 months at the time of the data lock. The vast majority of local and distant recurrences occur within 2 years of treatment in previous bladder-sparing studies of MIBC, although whether the same pattern and timing holds true for patients not undergoing cystectomy or receiving radiation is not well established<sup>2,26</sup>. Therefore, longer-term follow-up data are needed to fully understand the impact of this treatment regimen on disease control. The need for later cystectomy in a subset of patients developing local recurrence after a cCR raises the question of whether all patients achieving a cCR should receive (chemo)radiation to further optimize the likelihood of bladder preservation. The complex interplay of issues related to organ preservation, cancer control and potential over-treatment with such an approach warrants further consideration and investigation. Patient-reported outcome data would provide important additional context, but such information was not collected in our study.

A disconnect between clinical and pathological staging has often been cited as a barrier to TURBT plus systemic therapy as definitive treatment for MIBC, although many analyses highlighting such a disconnect have been retrospective and without uniform approaches to clinical response assessment<sup>35,36</sup>. Notwithstanding, a focus solely on the discrepancies between clinical and pathological staging may undermine the possibility that cystectomy at the time of local recurrence can achieve similar survival to immediate cystectomy in the subset of patients with subclinical disease not detected at initial clinical restaging. Many cCRs in patients who later develop local recurrence may indeed represent 'major pathological responses' accompanied by a distinct tumor biology and prognosis; the relatively favorable outcomes observed in our patients achieving a cCR and undergoing cystectomy for local recurrence is supportive of this notion. That cCRs do not align completely with pCRs is unlikely unique to bladder cancer. Even in locally advanced mismatch repair protein deficient (dMMR) colorectal tumors that are highly sensitive to immunotherapy, early data indicate a 100% cCR rate with immune checkpoint blockade in a small cohort of patients with dMMR rectal cancer deferring definitive surgery or chemoradiation, whereas a 67% pCR rate was observed with neoadjuvant immune checkpoint blockade followed by colectomy in dMMR colon cancer<sup>37,38</sup>. As defined in our study, cCR was associated with favorable bladder-intact and overall survival outcomes.

Integrating pre-treatment and on-treatment biomarkers could potentially refine selection of patients achieving a cCR after TURBT plus systemic therapy for omission of additional local therapy. Mutations in a pre-specified set of genes selected based on previous work<sup>15-22</sup> did not clearly enhance the ability of cCR to identify patients achieving prolonged bladder-intact survival. Our analysis is limited by the potential limitations of tumor-only DNA sequencing, the sample size and the paucity of pathogenic alterations in some genes (for example, *ATM*), although other studies have also been unable to confirm the relationship between these molecular alterations and clinical outcomes in patients with MIBC<sup>36,39</sup>. Ongoing clinical trials are prospectively



assessing the role of such molecular alterations in selecting patients for definitive treatment with TURBT plus chemotherapy (NCT02710734 and NCT03609216). Although VI-RADS<sup>25</sup>, a standardized approach to bladder cancer MRI imaging and reporting, was developed for initial

bladder cancer staging, our data highlight the prognostic impact of this system after systemic therapy for MIBC and the need for further study as a tool for selection of patients for bladder-sparing approaches in future trials.

**Fig. 4 | Association between peripheral blood immune populations as determined by mass cytometry (CyTOF) or peripheral blood or urine protein analytes and cCR or metastasis-free survival.** **a**, Timing of sample collection. **b**, Volcano plot for metastasis-free survival (MFS) based on C1D1 peripheral blood CyTOF data ( $n = 74$ ; patients without samples or outcome data were excluded) showing log-rank test (y axis) and Cox regression hazard ratio (x axis). **c**, Kaplan–Meier curves for CD4<sup>+</sup> naive T cells on C1D1 with Gehan–Breslow  $P$  values. **d**, Volcano plot for MFS based on C3D1 peripheral blood CyTOF data ( $n = 65$ ; patients without samples or outcome data were excluded) showing log-rank test (y axis) and Cox regression hazard ratio (x axis). **e**, Kaplan–Meier curves with Gehan–Breslow  $P$  values for CD8<sup>+</sup> naive T cells at C3D1. **f**, Volcano plot showing the differential expression of peripheral blood proteins on C1D1 ( $n = 71$ ; patients without samples or outcome data were excluded) according to cCR status ( $-\log_{10}(P$  value) in x axis and  $\log_2$  fold change calculated using moderated t-statistic). **g**, Volcano plot showing the differential expression of peripheral blood proteins on C3D1 ( $n = 65$ ; patients without samples or outcome

data were excluded) according to cCR status ( $-\log_{10}(P$  value) in x axis and  $\log_2$  fold change calculated using moderated t-statistic). **h**, Heat map showing the normalized expression (z-score) for peripheral blood proteins increased on C3D1 according to cCR status (hierarchically clustered using Ward’s algorithm). **i**, Volcano plot for MFS based on C1D1 expression of proteins showing log-rank test (y axis) and Cox regression hazard ratio (x axis). **j**, Kaplan–Meier curves for IL6 expression at C1D1 with Gehan–Breslow  $P$  values. **k**, Volcano plot for MFS based on C3D1 protein expression showing log-rank test (y axis) and Cox regression hazard ratio (x axis). **l**, Kaplan–Meier curves for ANGPT2 expression at C3D1 with Gehan–Breslow  $P$  values. **m**, Volcano plot for MFS based on urine proteins at time of clinical restaging ( $n = 59$ , patients without samples or outcome data were excluded) showing log-rank test (y axis) and Cox regression hazard ratio (x axis). For associations with cCR, adjustment for multiple comparisons was performed using the Benjamini–Hochberg method. **a** was created with BioRender. FDR, false discovery rate; HR, hazard ratio; Nivo, nivolumab; NA, not applicable.

Analysis of circulating immune parameters may facilitate biomarker discovery and insights related to the immunomodulatory effects of treatment. Mass cytometry analysis of PBMCs revealed that a higher abundance of pre-treatment naive CD4 T cells and on-treatment naive CD8 T cells was associated with longer metastasis-free and overall survival. Multiplex proteomic analysis of plasma revealed that increased on-treatment levels of cytotoxicity-related markers TRAIL, FasL and CD244 were associated with a higher likelihood of achieving a cCR. TRAIL and FasL are members of the tumor necrosis factor (TNF) superfamily and are expressed by immune effector cells, whereas CD244 is a surface receptor on natural killer (NK) cells and a subset of CD8 T cells<sup>40</sup>. Higher pre-treatment and on-treatment IL6 and ANGPT2 levels were associated with worse survival outcomes consistent with previous clinical and preclinical studies<sup>41,42</sup>. Overall, these findings are suggestive of a more robust NK cell and CD8 T cell immune response in patients with a more favorable response to treatment and underlying tumor-promoting inflammation in patients experiencing worse outcomes. The mechanisms by which on-treatment augmentation of immunity is achieved are currently being further explored, leveraging pre-treatment and post-treatment tumor tissue.

In our study, neoadjuvant gemcitabine, cisplatin, plus nivolumab after TURBT was associated with a cCR rate of 43%, and clinical response assessment identified patients with particularly favorable outcomes and facilitated bladder sparing. Genomic, imaging and immunological biomarkers have the potential to refine this treatment paradigm, but they require further investigation. These findings may help advance a more personalized approach to the management of MIBC.

## Online content

Any methods, additional references, Nature Portfolio reporting summaries, source data, extended data, supplementary information, acknowledgements, peer review information; details of author contributions and competing interests; and statements of data and code availability are available at <https://doi.org/10.1038/s41591-023-02568-1>.

## References

- Marqueen, K. E. et al. Early mortality in patients with muscle-invasive bladder cancer undergoing cystectomy in the United States. *JNCI Cancer Spectr.* **2**, pky075 (2018).
- Grossman, H. B. et al. Neoadjuvant chemotherapy plus cystectomy compared with cystectomy alone for locally advanced bladder cancer. *N. Engl. J. Med.* **349**, 859–866 (2003).
- Griffiths, G., Hall, R., Sylvester, R., Raghavan, D. & Parmar, M. K. International phase III trial assessing neoadjuvant cisplatin, methotrexate, and vinblastine chemotherapy for muscle-invasive bladder cancer: long-term results of the BA06 30894 trial. *J. Clin. Oncol.* **29**, 2171–2177 (2011).
- Flaig, T. W. et al. A randomized phase II study of coexpression extrapolation (COXEN) with neoadjuvant chemotherapy for bladder cancer (SWOG S1314; NCT02177695). *Clin. Cancer Res.* **27**, 2435–2441 (2021).
- Herr, H. W., Bajorin, D. F. & Scher, H. I. Neoadjuvant chemotherapy and bladder-sparing surgery for invasive bladder cancer: ten-year outcome. *J. Clin. Oncol.* **16**, 1298–301 (1998).
- Moran, G. W. et al. Systematic review and meta-analysis on the efficacy of chemotherapy with transurethral resection of bladder tumors as definitive therapy for muscle invasive bladder cancer. *Bladder Cancer* **3**, 245–258 (2017).
- Meyer, A. et al. The natural history of clinically complete responders to neoadjuvant chemotherapy for urothelial carcinoma of the bladder. *J. Urol.* **192**, 696–701 (2014).
- Solsona, E. et al. Bladder preservation in selected patients with muscle-invasive bladder cancer by complete transurethral resection of the bladder plus systemic chemotherapy: long-term follow-up of a phase 2 nonrandomized comparative trial with radical cystectomy. *Eur. Urol.* **55**, 911–921 (2009).
- deVere White, R. W. et al. A sequential treatment approach to myoinvasive urothelial cancer: a phase II Southwest Oncology Group trial (S0219). *J. Urol.* **181**, 2476–2480; discussion 2480–2481 (2009).
- Necchi, A. et al. Pembrolizumab as neoadjuvant therapy before radical cystectomy in patients with muscle-invasive urothelial bladder carcinoma (PURE-01): an open-label, single-arm, phase II study. *J. Clin. Oncol.* **36**, 3353–3360 (2018).
- Powles, T. et al. Clinical efficacy and biomarker analysis of neoadjuvant atezolizumab in operable urothelial carcinoma in the ABACUS trial. *Nat. Med.* **25**, 1706–1714 (2019).
- de Biasi, A. R., Villena-Vargas, J. & Adusumilli, P. S. Cisplatin-induced antitumor immunomodulation: a review of preclinical and clinical evidence. *Clin. Cancer Res.* **20**, 5384–5391 (2014).
- Gupta, S. et al. Results from BLASST-1 (Bladder Cancer Signal Seeking Trial) of nivolumab, gemcitabine, and cisplatin in muscle invasive bladder cancer (MIBC) undergoing cystectomy. *J. Clin. Oncol.* **38**, 439–439 (2020).
- Rose, T. L. et al. Phase II study of gemcitabine and split-dose cisplatin plus pembrolizumab as neoadjuvant therapy before radical cystectomy in patients with muscle-invasive bladder cancer. *J. Clin. Oncol.* **39**, 3140–3148 (2021).
- Iyer, G. et al. Multicenter prospective phase II trial of neoadjuvant dose-dense gemcitabine plus cisplatin in patients with muscle-invasive bladder cancer. *J. Clin. Oncol.* **36**, 1949–1956 (2018).
- Van Allen, E. M. et al. Somatic *ERCC2* mutations correlate with cisplatin sensitivity in muscle-invasive urothelial carcinoma. *Cancer Discov.* **4**, 1140–1153 (2014).



17. Liu, D. et al. Clinical validation of chemotherapy response biomarker *ERCC2* in muscle-invasive urothelial bladder carcinoma. *JAMA Oncol.* **2**, 1094–1096 (2016).
18. Plimack, E. R. et al. Defects in DNA repair genes predict response to neoadjuvant cisplatin-based chemotherapy in muscle-invasive bladder cancer. *Eur. Urol.* **68**, 959–967 (2015).
19. Iyer, G. et al. Association of DNA damage response (DDR) gene mutations (mts) and response to neoadjuvant cisplatin-based chemotherapy (chemo) in muscle-invasive bladder cancer (MIBC) patients (pts) enrolled onto SWOG S1314. *J. Clin. Oncol.* **40**, 4522 (2022).
20. Plimack, E. R. et al. S1314 correlative analysis of ATM, RB1, ERCC2, and FANCC mutations and pathologic complete response (pT0) at cystectomy after neoadjuvant chemotherapy (NAC) in patients with muscle invasive bladder cancer (MIBC): Implications for bladder preservation. *J. Clin. Oncol.* **40**, 4581 (2022).
21. Teo, M. Y. et al. Alterations in DNA damage response and repair genes as potential marker of clinical benefit from PD-1/PD-L1 blockade in advanced urothelial cancers. *J. Clin. Oncol.* **36**, 1685–1694 (2018).
22. Galsky, M. D. et al. Phase 2 trial of gemcitabine, cisplatin, plus ipilimumab in patients with metastatic urothelial cancer and impact of DNA damage response gene mutations on outcomes. *Eur. Urol.* **73**, 751–759 (2017).
23. Sha, D. et al. Tumor mutational burden (TMB) as a predictive biomarker in solid tumors. *Cancer Discov.* **10**, 1808 (2020).
24. Marabelle, A. et al. Association of tumour mutational burden with outcomes in patients with advanced solid tumours treated with pembrolizumab: prospective biomarker analysis of the multicohort, open-label, phase 2 KEYNOTE-158 study. *Lancet Oncol.* **21**, 1353–1365 (2020).
25. Panebianco, V. et al. Multiparametric magnetic resonance imaging for bladder cancer: development of VI-RADS (Vesical Imaging-Reporting and Data System). *Eur. Urol.* **74**, 294–306 (2018).
26. James, N. D. et al. Radiotherapy with or without chemotherapy in muscle-invasive bladder cancer. *N. Engl. J. Med.* **366**, 1477–1488 (2012).
27. Huddart, R. A. et al. Patient-reported quality of life outcomes in patients treated for muscle-invasive bladder cancer with radiotherapy ± chemotherapy in the BC2001 phase III randomised controlled trial. *Eur. Urol.* **77**, 260 (2020).
28. Efstathiou, J. A. et al. Late pelvic toxicity after bladder-sparing therapy in patients with invasive bladder cancer: RTOG 89-03, 95-06, 97-06, 99-06. *J. Clin. Oncol.* **27**, 4055–4061 (2009).
29. Schuettfort, V. M. et al. Incidence and outcome of salvage cystectomy after bladder sparing therapy for muscle invasive bladder cancer: a systematic review and meta-analysis. *World J. Urol.* **39**, 1757 (2021).
30. Galsky, M. D. et al. Atezolizumab with or without chemotherapy in metastatic urothelial cancer (IMvigor130): a multicentre, randomised, placebo-controlled phase 3 trial. *Lancet* **395**, 1547–1557 (2020).
31. Powles, T. et al. Pembrolizumab alone or combined with chemotherapy versus chemotherapy as first-line therapy for advanced urothelial carcinoma (KEYNOTE-361): a randomised, open-label, phase 3 trial. *Lancet Oncol.* **22**, 931–945 (2021).
32. Galsky, M. D. et al. Cisplatin (cis)-related immunomodulation and efficacy with atezolizumab (atezo) + cis- vs carboplatin (carbo)-based chemotherapy (chemo) in metastatic urothelial cancer (mUC). *Ann. Oncol.* **31**, S678–S724 (2021).
33. Powles, T. et al. Avelumab maintenance therapy for advanced or metastatic urothelial carcinoma. *N. Engl. J. Med.* **383**, 1218–1230 (2020).
34. Galsky, M. D. et al. Randomized double-blind phase II study of maintenance pembrolizumab versus placebo after first-line chemotherapy in patients with metastatic urothelial cancer. *J. Clin. Oncol.* **38**, 1797–1806 (2020).
35. Gray, P. J. et al. Clinical-pathologic stage discrepancy in bladder cancer patients treated with radical cystectomy: results from the national cancer data base. *Int. J. Radiat. Oncol. Biol. Phys.* **88**, 1048–56 (2014).
36. Becker, R. E. N. et al. Clinical restaging and tumor sequencing are inaccurate indicators of response to neoadjuvant chemotherapy for muscle-invasive bladder cancer. *Eur. Urol.* **79**, 364–371 (2020).
37. Cercek, A. et al. PD-1 blockade in mismatch repair-deficient, locally advanced rectal cancer. *N. Engl. J. Med.* **386**, 2363–2376 (2022).
38. Chalabi, M. et al. Neoadjuvant immune checkpoint inhibition in locally advanced MMR-deficient colon cancer: the NICHE-2 study. *Ann. Oncol.* **33** <https://doi.org/10.1016/j.annonc.2022.08.016> (2022).
39. Gil-Jimenez, A. et al. Assessment of predictive genomic biomarkers for response to cisplatin-based neoadjuvant chemotherapy in bladder cancer. *Eur. Urol.* **83**, 313–317 (2023).
40. Rossin, A., Miloro, G. & Hueber, A. O. TRAIL and FasL functions in cancer and autoimmune diseases: towards an increasing complexity. *Cancers (Basel)* **11**, 639 (2019).
41. Huseni, M. A. et al. CD8<sup>+</sup> T cell-intrinsic IL-6 signaling promotes resistance to anti-PD-L1 immunotherapy. *Cell Rep. Med.* **4**, 100878 (2023).
42. Park, H.-R. et al. Angiopoietin-2-dependent spatial vascular destabilization promotes T-cell exclusion and limits immunotherapy in melanoma. *Cancer Res.* **83**, 1968–1983 (2023).

**Publisher's note** Springer Nature remains neutral with regard to jurisdictional claims in published maps and institutional affiliations.

**Open Access** This article is licensed under a Creative Commons Attribution 4.0 International License, which permits use, sharing, adaptation, distribution and reproduction in any medium or format, as long as you give appropriate credit to the original author(s) and the source, provide a link to the Creative Commons license, and indicate if changes were made. The images or other third party material in this article are included in the article's Creative Commons license, unless indicated otherwise in a credit line to the material. If material is not included in the article's Creative Commons license and your intended use is not permitted by statutory regulation or exceeds the permitted use, you will need to obtain permission directly from the copyright holder. To view a copy of this license, visit <http://creativecommons.org/licenses/by/4.0/>.

© The Author(s) 2023

**Matthew D. Galsky**<sup>1,2</sup>✉, **Siamak Daneshmand**<sup>3</sup>, **Sudeh Izadmehr**<sup>4</sup>, **Edgar Gonzalez-Kozlova**<sup>4</sup>, **Kevin G. Chan**<sup>5</sup>, **Sara Lewis**<sup>6</sup>, **Bassam El Achkar**<sup>6</sup>, **Tanya B. Dorff**<sup>7</sup>, **Jeremy Paul Cetnar**<sup>8</sup>, **Brock O. Neil**<sup>9</sup>, **Anishka D'Souza**<sup>10</sup>, **Ronac Mamtani**<sup>11</sup>, **Christos Kyriakopoulos**<sup>12</sup>, **Tomi Jun**<sup>13,25</sup>, **Mahalya Gogerly-Moragoda**<sup>1</sup>, **Rachel Brody**<sup>2,14</sup>, **Hui Xie**<sup>15</sup>, **Kai Nie**<sup>15</sup>, **Geoffrey Kelly**<sup>15</sup>, **Amir Horwitz**<sup>2,16</sup>, **Yayoi Kinoshita**<sup>14</sup>, **Ethan Ellis**<sup>17,18</sup>, **Yohei Nose**<sup>16</sup>, **Giorgio Ioannou**<sup>16</sup>, **Rafael Cabal**<sup>16</sup>, **G. Kenneth Haines**<sup>19</sup>, **Li Wang**<sup>1,20</sup>, **Kent W. Mouw**<sup>21</sup>, **Robert M. Samstein**<sup>22</sup>, **Reza Mehrazin**<sup>23</sup>, **Nina Bhardwaj**<sup>2,15,16</sup>, **Menggang Yu**<sup>24</sup>, **Qianqian Zhao**<sup>24</sup>, **Seunghee Kim-Schulze**<sup>2,15,16</sup>, **Robert Sebra**<sup>2,17,18</sup>, **Jun Zhu**<sup>1,20</sup>, **Sacha Gnjatich**<sup>2,15,16,26</sup>, **John Sfakianos**<sup>23,26</sup> & **Sumanta K. Pal**<sup>2,26</sup>

<sup>1</sup>Division of Hematology and Medical Oncology, Icahn School of Medicine at Mount Sinai, New York, NY, USA. <sup>2</sup>Tisch Cancer Institute, Icahn School of Medicine at Mount Sinai, New York, NY, USA. <sup>3</sup>Department of Urology, Keck School of Medicine of USC, Norris Comprehensive Cancer Center, Los Angeles, CA, USA. <sup>4</sup>Department of Oncological Sciences, Tisch Cancer Institute, Icahn School of Medicine at Mount Sinai, New York, NY, USA. <sup>5</sup>Department of Urology, City of Hope Comprehensive Cancer Center, Duarte, CA, USA. <sup>6</sup>Department of Radiology, Tisch Cancer Institute, Icahn School of Medicine at Mount Sinai, New York, NY, USA. <sup>7</sup>Department of Medical Oncology & Therapeutics, City of Hope Comprehensive Cancer Center, Duarte, CA, USA. <sup>8</sup>Division of Hematology and Medical Oncology, Oregon Health and Science University, Portland, OR, USA. <sup>9</sup>Department of Urology, University of Utah, Salt Lake City, UT, USA. <sup>10</sup>Division of Hematology and Medical Oncology, Keck School of Medicine of USC, Norris Comprehensive Cancer Center, Los Angeles, CA, USA. <sup>11</sup>Division of Hematology and Medical Oncology, University of Pennsylvania Abramson Cancer Center, Philadelphia, PA, USA. <sup>12</sup>Division of Hematology and Medical Oncology, University of Wisconsin Carbone Cancer Center, Madison, WI, USA. <sup>13</sup>Genentech, South San Francisco, CA, USA. <sup>14</sup>Department of Pathology, Tisch Cancer Institute, Icahn School of Medicine at Mount Sinai, New York, NY, USA. <sup>15</sup>Human Immune Monitoring Center, Icahn School of Medicine at Mount Sinai, New York, NY, USA. <sup>16</sup>Precision Immunology Institute, Icahn School of Medicine at Mount Sinai, New York, NY, USA. <sup>17</sup>Department of Genetics and Genomic Sciences, Icahn School of Medicine at Mount Sinai, New York, NY, USA. <sup>18</sup>Icahn Institute for Data Science and Genomic Technology, Icahn School of Medicine at Mount Sinai, New York, NY, USA. <sup>19</sup>Department of Pathology, Molecular and Cell-based Medicine, Icahn School of Medicine at Mount Sinai, New York, NY, USA. <sup>20</sup>Gene Dx, Stamford, CT, USA. <sup>21</sup>Department of Radiation Oncology, Dana-Farber Cancer Institute/Brigham & Women's Hospital, Harvard Medical School, Boston, MA, USA. <sup>22</sup>Department of Radiation Oncology, Tisch Cancer Institute, Icahn School of Medicine at Mount Sinai, New York, NY, USA. <sup>23</sup>Department of Urology, Tisch Cancer Institute, Icahn School of Medicine at Mount Sinai, New York, NY, USA. <sup>24</sup>Department of Biostatistics and Medical Informatics, University of Wisconsin Carbone Cancer Center, Madison, WI, USA. <sup>25</sup>Present address: Formerly with the Icahn School of Medicine at Mount Sinai, New York, NY, USA. <sup>26</sup>These authors contributed equally: Sacha Gnjatic, John Sfakianos, Sumanta K. Pal.

✉ e-mail: [matthew.galsky@mssm.edu](mailto:matthew.galsky@mssm.edu)

## Methods

### Study design

HCRN GU 16–257 is phase 2, investigator-initiated, multicenter clinical trial. Cisplatin-eligible patients with MIBC enrolled at seven medical centers received treatment with gemcitabine, cisplatin, plus nivolumab (Fig. 1a). Clinical restaging was performed after cycle 4. Patients achieving a cCR were offered the option to proceed with radical cystectomy versus retain their bladder and receive eight additional doses of nivolumab followed by surveillance. Patients not achieving a cCR were recommended to proceed with radical cystectomy. The surveillance schedule is outlined in the protocol (Supplementary Information). The study was conducted in accordance with the Declaration of Helsinki. The protocol was approved by local ethics committees at the Icahn School of Medicine at Mount Sinai, the City of Hope Comprehensive Cancer Center, the Huntsman Cancer Institute University of Utah, the Oregon Health and Science University, the Penn Medicine Abramson Cancer Center, the Rutgers Cancer Institute of New Jersey, the University of Southern California and the University of Wisconsin, and written informed consent was provided by all patients before enrollment. The trial was registered at ClinicalTrials.gov (NCT03558087).

### Patients

#### Inclusion criteria:

- Written informed consent and HIPAA authorization for release of personal health information before registration
- Age  $\geq 18$  years at the time of consent
- Eastern Cooperative Oncology Group (ECOG) performance status of  $\leq 1$  within 28 d before registration
- Histological evidence of clinically localized muscle-invasive UC of the bladder (that is, cT2N0M0)
- Candidate for cystectomy as per treating physician
- Adequate organ function
- Adequate archival tissue identified at screening (that is, at least 15 unstained slides or paraffin block)
- Women of childbearing potential must have a negative serum or urine pregnancy test within 7 d before cycle 1, day 1.

#### Exclusion criteria:

- Prior treatment with systemic chemotherapy for muscle-invasive UC of the bladder
- Active infection requiring systemic therapy
- Pregnant or breastfeeding
- Any serious or uncontrolled medical disorder that, in the opinion of the investigator, may increase the risk associated with study participation or study drug administration, impair the ability of the subject to receive protocol therapy or interfere with the interpretation of study results
- Prior malignancy active within the previous 3 years except for locally curable cancers that have been apparently cured
- Subjects with active, known or suspected autoimmune disease. Subjects with vitiligo, type I diabetes mellitus, residual hypothyroidism due to autoimmune condition requiring only hormone replacement, psoriasis not requiring systemic treatment or conditions not expected to recur in the absence of an external trigger are permitted to enroll.
- Subjects with a condition requiring systemic treatment with either corticosteroids ( $>10$  mg daily prednisone equivalents) or other immunosuppressive medications within 14 d of study drug administration. Inhaled or topical steroids and adrenal replacement doses  $>10$  mg daily prednisone equivalents are permitted in the absence of active autoimmune disease.
- Prior treatment with an anti-PD-1, anti-PD-L1, anti-PD-L2, anti-CTLA-4 antibody or any other antibody or drug specifically targeting T cell co-stimulation or immune checkpoint pathways

- Grade  $\geq 2$  neuropathy (National Cancer Institute Common Terminology Criteria for Adverse Events (NCI CTCAE) version 4.03)
- Prior radiation therapy for bladder cancer
- Positive test for hepatitis B virus surface antigen (HBV sAg) or hepatitis C virus RNA or hepatitis C antibody (HCV antibody), indicating acute or chronic infection
- Known history of testing positive for HIV or known AIDS
- Evidence of interstitial lung disease or active, non-infectious pneumonitis

### Treatment

Cycles 1–4 of treatment included gemcitabine  $1,000 \text{ mg m}^{-2}$  on days 1 and 8, cisplatin  $70 \text{ mg m}^{-2}$  on day 1 and nivolumab  $360 \text{ mg}$  on day 1, all administered intravenously in 21-d cycles. Patients achieving a cCR and opting to proceed without cystectomy received single-agent nivolumab  $240 \text{ mg}$  intravenously every 2 weeks for eight doses. Patients with a cCR and forgoing immediate cystectomy then proceeded with surveillance using the following strategy: urine cytology every 3 months for years 1–2, every 6 months for years 2–4 and annually for year 5; cystoscopy every 3 months for years 1–2, every 6 months for years 2–4 and annually for year 5; and cross-sectional imaging of the chest, abdomen and pelvis every 3 months to year 1.5, every 6 months to year 3 and annually to year 5. Patients with an invasive local recurrence were recommended to proceed with cystectomy.

Adverse events were graded according to the NCI CTCAE version 4.03. Adverse events were managed according to algorithms based on the specific toxicity as defined in the protocol.

### Clinical restaging and cCR definition

After cycle 4 of gemcitabine, cisplatin, plus nivolumab, patients underwent clinical restaging including MRI of the abdomen and pelvis or CT if MRI was contraindicated and CT of the chest, rigid cystoscopy with biopsies and urine cytology. Transurethral resection of any visible tumor and/or the prior tumor site was performed. In addition, biopsies were obtained from the following sites: trigone, left, right, anterior, posterior and dome. In men, prostatic urethral biopsies were performed. A cCR was defined as meeting all of the following: (1) no evidence of malignancy on biopsy with the exception of low-grade papillary (Ta) tumors; (2) no malignant cells on urine cytology; and (3) no evidence of local or metastatic disease on cross-sectional imaging. Residual bladder wall changes on cross-sectional imaging were interpreted by the treating investigator in consultation with the local radiologist and in the context of the bladder biopsy results. A blinded post hoc central review of the restaging MRI scans was completed by two study radiologists (S.L. and B.E.A.) to assign a VI-RADS<sup>25</sup> score—a standardized approach to bladder cancer MRI assessment and reporting. Inter-rater agreement was assessed using the weighted kappa statistic<sup>43</sup>. The VI-RADS value from the more experienced reviewer (S.L.) was used when there was not agreement.

### PD-L1 immunohistochemistry on baseline TURBT specimens

Immunohistochemistry for PD-L1 was performed in the Department of Pathology at the Mount Sinai Hospital using the 22C3 antibody clone. PD-L1 expression was quantified by a single genitourinary pathologist (G.K.H.) blinded to clinical outcome data using the combined positive score (CPS), defined as the percentage of PD-L1-expressing tumor and infiltrating immune cells relative to the total number of tumor cells. A cutpoint of CPS  $\geq 10$  was used to define 'high' PD-L1 expression as per previous studies in UC<sup>44</sup>.

### DNA sequencing of baseline TURBT specimens

Archival baseline TURBT tissue underwent tumor-only targeted DNA sequencing using the Illumina NextSeq platform (Caris Life Sciences). An Agilent custom-designed SureSelect XT assay (Caris MI TumorSeek 592-Gene NGS Panel) was used to enrich 591 whole-gene

targets. Sequencing and gene variant calling were carried out as previously described; the pipeline automatically filters out known common germline population variants (that is, from databases such as dbSNP) and flags pathogenic mutations that are potentially germline<sup>45</sup>. To address artifacts that might be introduced in formalin-fixed, paraffin-embedded (FFPE) samples, samples with low depth or unusual variant composition are flagged for review and potential resequencing. Multiple non-reference reads (>20) were needed to support variant calling. In addition, if forward and reverse reads at the single-nucleotide polymorphism (SNP) locations largely deviated from balance, the variants were filtered out. For the flanking regions around the SNPs in the genes in Fig. 3, the mean sequencing depth was 1,243 (137–6,407). Mutations were considered pathogenic or presumed pathogenic according to guidelines set by the American College of Medical Genetics and the Association for Molecular Pathology<sup>46</sup>. Mutations in *ERCC2* were further annotated incorporating the results of published functional assays (K.M.)<sup>47</sup>. TMB was calculated using only missense mutations as previously described<sup>48</sup>.

### Mass cytometry (CyTOF)

Mass cytometry (CyTOF) was performed on PBMCs obtained on cycle 1, day 1 and cycle 3, day 1 of treatment. PBMCs were stained with the CyTOF antibody panel detailed in Supplementary Table 5. All antibodies were either purchased pre-conjugated from Fluidigm or conjugated in-house (using commercial X8 polymer conjugation kits purchased from Fluidigm) at the Human Immune Monitoring Center (HIMC), Icahn School of Medicine at Mount Sinai. All in-house conjugated antibodies were titrated and validated on healthy donor PBMCs. For longitudinal monitoring of phenotypic changes, cells from selected timepoints were thawed, counted and assessed for viability using the Nexcelom Cellaca Automated Cell Counter (Nexcelom Bioscience) along with acridine orange/propidium iodine staining (Nexcelom Bioscience). For sample timepoint batching, live-cell CyTOF barcoding was performed using anti-B2M antibodies conjugated to unique cadmium isotopes. Rhodium-103 viability and Human TruStain FcX staining were performed simultaneously at room temperature for 30 min. After cell washing in flow cytometry buffer (1× PBS + 0.2% BSA + 0.05% Na<sub>2</sub>S<sub>2</sub>O<sub>8</sub>), cells were stained with a cocktail of surface antibodies (Supplementary Table 5). Surface-stained cells were further fixed with 1.6% formaldehyde. Each sample was then barcoded with the CyTOF Cell-ID 20-Plex Palladium Barcoding Kit (Fluidigm), pooled and fixed in freshly made 4% paraformaldehyde containing 125 nM intercalator-Ir (Fluidigm) and 300 nM OsO<sub>4</sub> (Acros Organics) and stored at –80 °C in FBS + 10% DMSO. Samples were washed with cell staining buffer (Fluidigm) and re-suspended in CAS buffer containing EQ normalization beads (Fluidigm) and acquired on a Helios mass cytometer equipped with a wide-bore sample injector at an event rate of <400 events per second. After acquisition, repeat acquisitions of the same sample were concatenated and normalized using Fluidigm software. The FCS file was further cleaned using the HIMC internal pipeline. The pipeline removed any aberrant acquisition time windows of 3 s where the cell sampling event rate was too high or too low (2 s.d. from the mean). EQ normalization beads spiked into every acquisition and used for normalization were removed, along with events that had low DNA signal intensity. The pipeline also was used to demultiplex the cleaned and pooled FCS files into constituent single-sample files. The cosine similarity of every cell's Pd barcoding channels to every possible barcode used in a batch was calculated and then was assigned to its highest similarity barcode. Once the cell had been assigned to a sample barcode, the difference between its highest and second highest similarity scores was calculated and used as a signal-to-noise metric. Any cells with low signal to noise were flagged as multiplets and removed from that sample. Finally, acquisition multiplets were removed based on the Gaussian parameters Residual and Offset acquired by the Helios mass cytometer.

Astrolabe was employed for automated computational annotation (Astrolabe Diagnostics). CyTOF analysis was performed using Astrolabe annotated data and statistical modeling with R. The data were loaded into R using the package 'orloj'. Astrolabe gating strategies were manually reviewed for a subset of samples. Data were uploaded to CytoBank for quality control analysis and visualization.

### Multiplex protein immunoassay

Plasma (cycle 1, day 1 and cycle 3, day 1) and urine (at time of restaging) were analyzed using the Olink Immuno-Oncology panel, which measures 92 proteins involved in immune response and tumor biology, using the Olink multiplex assay (Olink Bioscience) according to the manufacturer's instructions. The Olink panel uses proximity extension assay technology, which relies on pairs of DNA-labeled antibodies that bind to target proteins and generate unique reporter molecules that can be quantified by real-time polymerase chain reaction. The Olink panel provides normalized protein expression units (NPX), which are log<sub>2</sub>-transformed values proportional to protein concentration. One NPX difference is equal to a doubling of the protein concentration.

### Statistical analysis

The co-primary objectives of the study were to (1) estimate the cCR rate with gemcitabine, cisplatin, plus nivolumab and (2) assess the positive predictive value of cCR for a composite outcome measure of (1) 2-year metastasis-free survival in patients achieving a cCR and opting to not undergo immediate cystectomy or (2) <pT1N0 in patients with a cCR who opted for immediate cystectomy. Secondary objectives included assessing the association between genomic alterations in a pre-specified panel of genes detected in pre-treatment TURBT tissue (*ERCC2*, *ATM*, *RBI* and *FANCC*<sup>15–22</sup>) as well as TMB (using an established cutpoint of ≥10 mut/Mb<sup>23,24</sup>) and clinical outcomes. Additional secondary objectives included safety, metastasis-free survival, overall survival and bladder-intact survival.

The sample size was based on the following assumptions: (1) patients without a cCR would not be suitable to forgo cystectomy; (2) ~40% of enrolled patients would achieve a cCR; and (3) ~35% of enrolled patients would achieve the composite outcome measure. Therefore, our assumption implied that the negative predictive value of a cCR would be 1. The sample size was based on the CI width of the positive predictive value of cCR for the composite outcome measure and generated such that the lower bound of the 95% one-sided CI exceeded 80%. This required enrollment of 68 patients, and the sample size was increased to 76 to account for potential missing data.

Rates were calculated using percentages and compared among different groups using Fisher's exact test. Time-to-event outcomes were analyzed using the Kaplan–Meier method and log-rank test. When comparing time-to-event outcomes for restaging cCR status and restaging VI-RADS, landmark analyses were conducted using the restaging times as the landmark time (that is, time 0). *P* values less than 0.05 were deemed statistically significant.

For analysis of multiplex protein immunoassay (Olink) data, the data were normalized with the reference samples using R software. The data distribution per sample was compared, and samples were inspected with warnings after NPX conversion. For CyTOF analysis, the data were normalized to percent of cell abundance and 95th percentile of surface protein expression. For Olink and CyTOF, differential protein expression and differential cell abundance, respectively, were calculated using a mixed effect linear model strategy to adjust for relevant clinical variables (ECOG performance status) and demographics (age, race and gender). First, the variance profiles and data distributions were explored to identify potential biases and assess the effect of relevant covariates in the analysis using the packages lme4, variancePartition and Dream. For Olink and CyTOF, quality control analysis served to identify biases such as low detection and poor sample quality. The filters included removing variables with more than 40–70% not available

or under the limit of detection values. The variables were verified as linearly independent such that there was no redundancy in the data. After quality control, individual expression or abundance was modeled as a function of relevant endpoints and covariates. Differential expression or abundance analyses were performed applying a contrast matrix to each regression model (one per endpoint) and using the moderated *t*-statistic or log odds when appropriate. False discovery rate adjustment was performed on resulting *P* values for multiple testing as described by Benjamini and Hochberg<sup>49</sup>. The Kaplan–Meier method was used to estimate metastasis-free and overall survival. Comparisons of time-to-event distributions between groups were made with the log-rank and Gehan–Breslow tests. Univariable Cox proportional hazard regression models were used to estimate the hazard ratios and corresponding 95% CIs for metastasis-free and overall survival. Landmark analyses were employed for cycle 3, day 1 or restaging timepoints. All statistical analyses were performed using SAS software version 9.4 (SAS Institute) and RStudio version 4.0.0 (R Core Team).

### Reporting summary

Further information on research design is available in the Nature Portfolio Reporting Summary linked to this article.

### Data availability

In accordance with NIH's Genomic Data Sharing Policy, the DNA sequencing data used to support the findings of this study have been deposited under controlled access in the database of Genotypes and Phenotypes (dbGaP) under accession number phs0003372. Genomic, clinical, mass cytometry and protein analyte data from this study used to support this publication will be made available upon reasonable request from a qualified medical or scientific professional for the specific purpose laid out in that request and may include de-identified individual participant data. Requests for secondary use of this data will require completing a data use agreement ([https://osp.od.nih.gov/wp-content/uploads/Model\\_DUC.pdf](https://osp.od.nih.gov/wp-content/uploads/Model_DUC.pdf)) and submitting a data access request to the NIH.

### References

43. Cohen, J. Weighted kappa: nominal scale agreement provision for scaled disagreement or partial credit. *Psychol. Bull.* **70**, 213–220 (1968).
44. Balar, A. V. et al. First-line pembrolizumab in cisplatin-ineligible patients with locally advanced and unresectable or metastatic urothelial cancer (KEYNOTE-052): a multicentre, single-arm, phase 2 study. *Lancet Oncol.* **18**, 1483–1492 (2017).
45. Tokunaga, R. et al. Molecular profiling of appendiceal adenocarcinoma and comparison with right-sided and left-sided colorectal cancer. *Clin. Cancer Res.* **25**, 3096–3103 (2019).
46. Richards, S. et al. Standards and guidelines for the interpretation of sequence variants: a joint consensus recommendation of the American College of Medical Genetics and Genomics and the Association for Molecular Pathology. *Genet. Med.* **17**, 405 (2015).
47. Li, Q. et al. *ERCC2* helicase domain mutations confer nucleotide excision repair deficiency and drive cisplatin sensitivity in muscle-invasive bladder cancer. *Clin. Cancer Res.* **25**, 977–988 (2019).
48. Vanderwalde, A., Spetzler, D., Xiao, N., Gatalica, Z. & Marshall, J. Microsatellite instability status determined by next-generation sequencing and compared with PD-L1 and tumor mutational burden in 11,348 patients. *Cancer Med.* **7**, 746–756 (2018).
49. Benjamini, Y. & Hochberg, Y. Controlling the false discovery rate: a practical and powerful approach to multiple testing. *J. R. Stat. Soc.* **57**, 289–300 (1995).

### Acknowledgements

This trial was funded by Bristol Myers Squibb, and translational analyses were supported by the V Foundation for Cancer Research

T2019-011 (M.D.G. and J.Z.). Scientific and financial support for the CIMAC-CIDC Network is provided through NCI Cooperative Agreements U24CA224319 (to the Icahn School of Medicine at Mount Sinai CIMAC), U24CA224331 (to the Dana-Farber Cancer Institute CIMAC), U24CA224285 (to the MD Anderson Cancer Center CIMAC) and U24CA224316 (to the CIDC at the Dana-Farber Cancer Institute). The content is solely the responsibility of the authors and does not necessarily represent the official views of the National Institutes of Health. Study GU16-257 was additionally supported through the Foundation for the National Institutes of Health (FNIH), in partnership with Friends of Cancer Research. Scientific and financial support for the Partnership for Accelerating Cancer Therapies public–private partnership are made possible through funding support provided to the FNIH by AbbVie, Amgen, Boehringer Ingelheim, Bristol Myers Squibb, Celgene, Genentech, Gilead, GlaxoSmithKline, Janssen, Novartis Institutes for Biomedical Research, Pfizer and Sanofi. Additional support for investigators included P30 CA196521 (M.D.G. and S.G.); R01 CA249175 (M.D.G.); T32 CA078207 (S.I.); NIH/LRP (S.I.); and U01 DK124165 (S.G.). This work used the services of the Tisch Cancer Institute Biorepository and Pathology Core.

### Author contributions

Conception and design: M.D.G. Financial support: M.D.G. Administrative support: M.D.G. and S.I. Provision of study materials: M.D.G., S.D., K.G.C., T.B.D., J.P.C., B.O., A.D., R.M., C.K., R.B., H.X., K.N., Y.K., E.E., R.M., S.G., J.S. and S.K.P. Collection and assembly of data: M.D.G., S.D., S.I., E.G., K.G.C., S.L., B.E., T.B.D., J.P.C., B.O., A.D., R.M., C.K., T.J., M.G., R.B., H.X., K.N., Y.K., E.E., Y.N., G.I., R.C., G.K.H., R.M., M.Y., Q.Z., S.K., R.S., J.Z., S.G., J.S. and S.K.P. Data analysis and interpretation: M.D.G., S.D., S.I., E.G., K.G.C., S.L., B.E., T.B.D., J.P.C., B.O., A.D., R.M., C.K., T.J., G.K., A.H., Y.N., G.I., R.C., L.W., K.W.M., R.M.S., N.B., Q.Z., S.K., R.S., J.Z., S.G., J.S. and S.K.P. Manuscript writing: M.D.G., E.G., S.L., T.J., Y.K., M.Y., Q.Z., S.K., R.S. and J.Z. Final approval of manuscript: M.D.G., S.D., S.I., E.G., K.G.C., S.L., B.E., T.B.D., J.P.C., B.O., A.D., R.M., C.K., T.J., M.G., R.B., H.X., K.N., G.K., A.H., Y.K., E.E., Y.N., G.I., R.C., G.K.H., L.W., K.W.M., R.M.S., R.M., N.B., M.Y., Q.Z., S.K., R.S., J.Z., S.G., J.S. and S.K.P. Accountable for all aspects of the work: M.D.G.

### Competing interests

M.D.G. has received research funding from Bristol Myers Squibb, Novartis, Dendreon, AstraZeneca, Merck and Genentech. He has served as a consultant to Bristol Myers Squibb, Merck, Genentech, AstraZeneca, Pfizer, EMD Serono, SeaGen, Janssen, Numab, Dragonfly, GlaxoSmithKline, Basilea, UroGen, Rapta Therapeutics, Alligator, Silverback, Fujifilm, Curis, Gilead, Bicycle, Asieris, Abbvie and Analog Devices. S.D. has served as a consultant to Janssen, Ferring, Photocure, Taris, Pacific Edge, QED, Abbvie, Janssen, Bristol Myers Squibb, Sesen, Protara, Pfizer and CG Oncology. T.B.D. has served as a consultant to Astellas, AstraZeneca, Bayer, Janssen and Sanofi. R.M. has served as a consultant to Bristol Myers Squibb, Roche, Astellas and Seattle Genetics and has received research funding from Merck and Astellas. C.K. has served as a consultant to Exelixis, Sanofi, AVEO, EMD Serono and Janssen and has received research funding from Sanofi, Gilead Sciences, AstraZeneca, ESSA Pharma, Pionyr and Incyte. He owns stock in Biogen and Epic Systems. T.J. is an employee of Genentech. A.H. has served as a consultant to HTG Molecular Diagnostics and Immunorizon. L.W. is an employee of GeneDx. K.W.M. has served as a consultant to EMD Serono, Pfizer, UroGen and Riva Therapeutics, has received research support from Pfizer and Novo Ventures, has equity in Riva Therapeutics, has received writing fees from UpToDate and has received speaking fees from OncoLive. He is named on an institutional patent filed on mutational signatures of DNA repair deficiency. N.B. has served as a consultant to Apricity, BreakBio, Carisma Therapeutics, CureVac, Genentech, Novartis,

Primevax, Tempest Therapeutics, Dragonfly Therapeutics, BioNTech, Genotwin and Rome Therapeutics. She has received research support from Harbour Biomed Sciences and Regeneron. J.Z. is an employee of GeneDx. S.G. received research funding from Boehringer Ingelheim, Bristol Myers Squibb, Celgene, Genentech, Regeneron and Takeda. J.S. has served as a consultant or advisor for Natera, Pacific Edge, Merck, Urogen and Janssen. S.K.P. has received travel support from CRISPR Therapeutics and Ipsen. All remaining authors declare no competing interests.

### Additional information

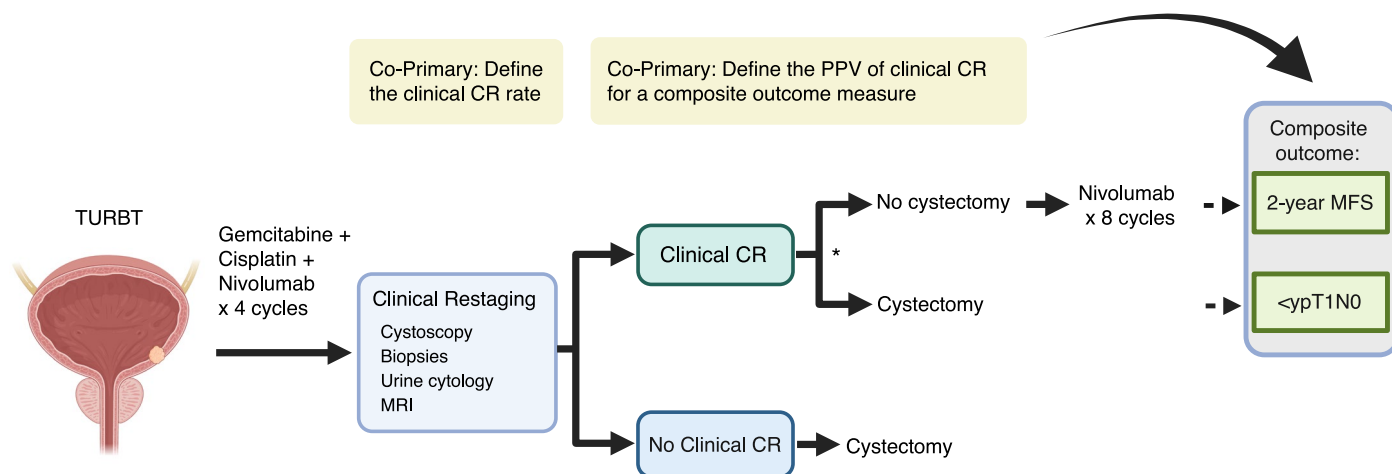
**Extended data** is available for this paper at <https://doi.org/10.1038/s41591-023-02568-1>.

**Supplementary information** The online version contains supplementary material available at <https://doi.org/10.1038/s41591-023-02568-1>.

**Correspondence and requests for materials** should be addressed to Matthew D. Galsky.

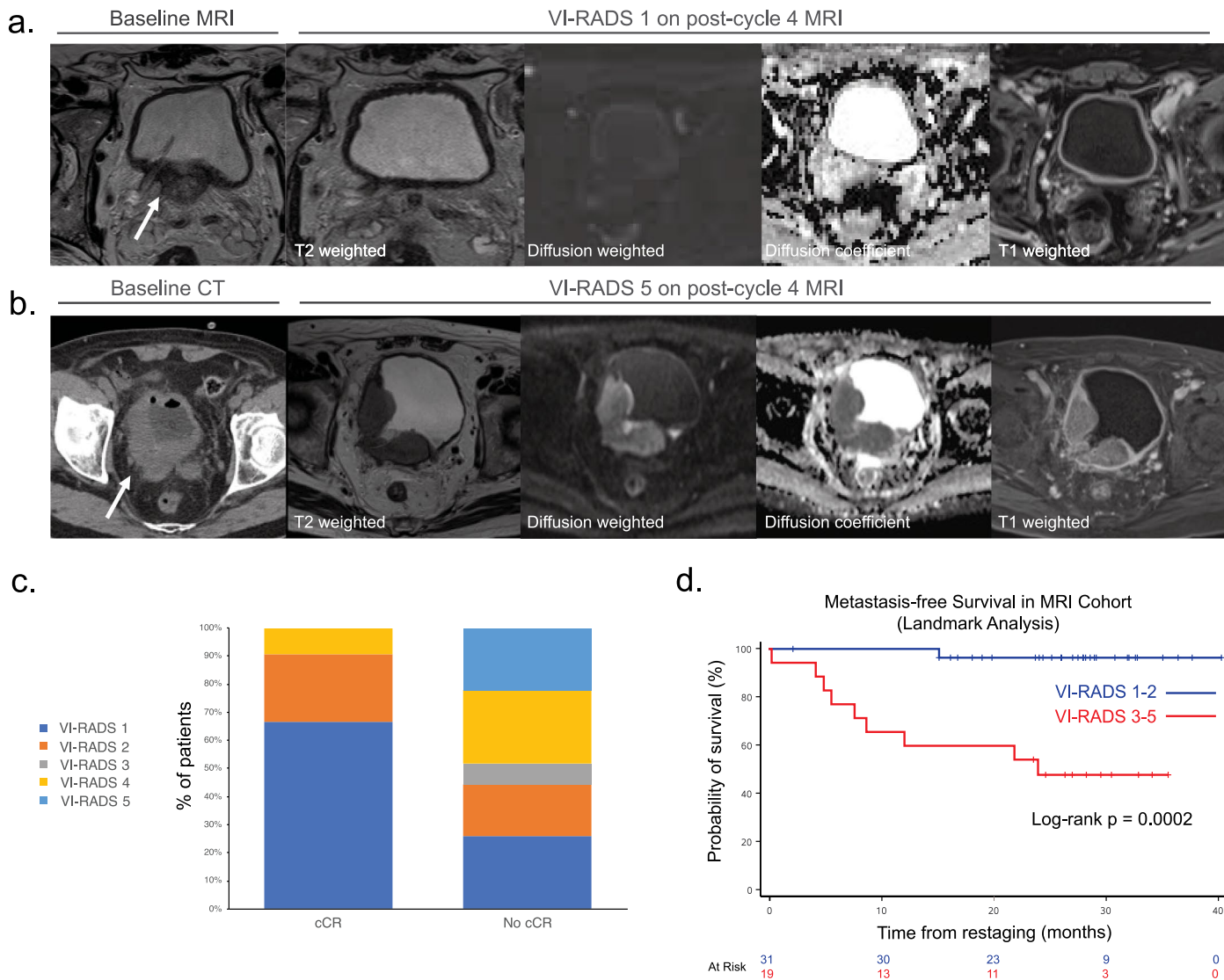
**Peer review information** *Nature Medicine* thanks Michiel van der Heijden, Roger Li, Lars Dyrskjøt and the other, anonymous, reviewer(s) for their contribution to the peer review of this work. Primary Handling Editor: Saheli Sadanand, in collaboration with the *Nature Medicine* team.

**Reprints and permissions information** is available at [www.nature.com/reprints](http://www.nature.com/reprints).



**Extended Data Fig. 1 | Schematic representation of the design of HCRN GU16-257.** Patients with muscle-invasive urothelial cancer of the bladder diagnosed based on standard of care TURBT (transurethral resection of bladder tumor) received four cycles of gemcitabine, cisplatin, plus nivolumab followed by clinical restaging consisting of cystoscopy with biopsies, urine cytology, and imaging including MRI (magnetic resonance imaging) of the bladder (or computed tomography scan if MRI was contraindicated). Patients achieving a clinical complete response (cCR) were offered the option to proceed with

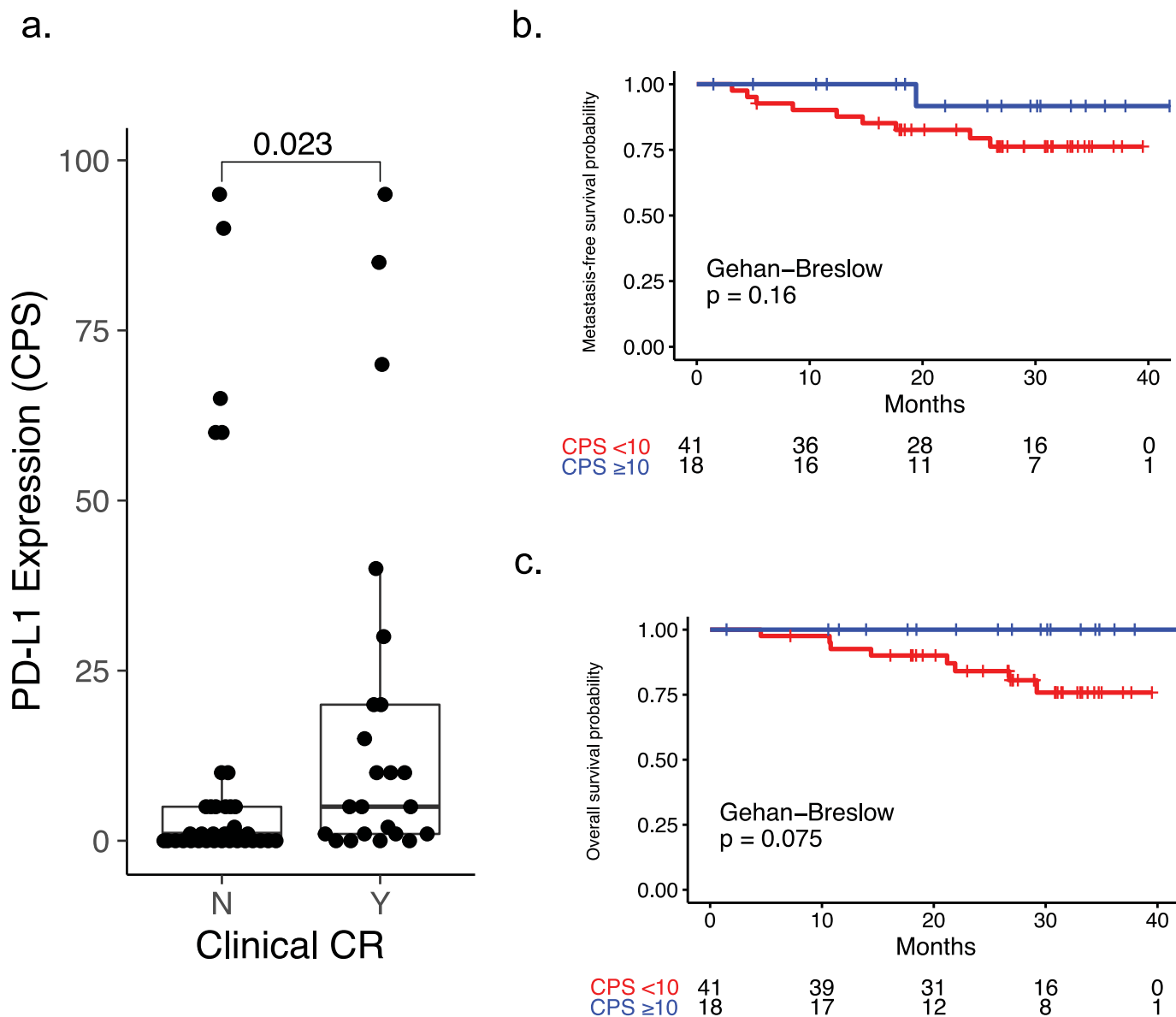
immediate cystectomy versus proceed without cystectomy and receive an additional 4 months of single-agent nivolumab followed by surveillance. Patients without a cCR were recommended to undergo immediate cystectomy. The primary objectives were to estimate the cCR rate and to assess the positive predictive value (PPV) of cCR for a composite outcome measure (MFS, metastasis-free survival). \*Patients achieving a clinical CR were offered the option to forgo cystectomy or proceed with immediate cystectomy.



**Extended Data Fig. 2 | Vesical Imaging-Reporting And Data System (VI-RADS) scoring of bladder magnetic resonance imaging (MRI) post-treatment with gemcitabine, cisplatin, plus nivolumab and association with clinical outcomes. (a)** Representative baseline image demonstrating posterior bladder wall mass and post- gemcitabine, cisplatin, plus nivolumab MRI sequences scored as VI-RADS 1. **(b)** Representative baseline image demonstrating posterior bladder

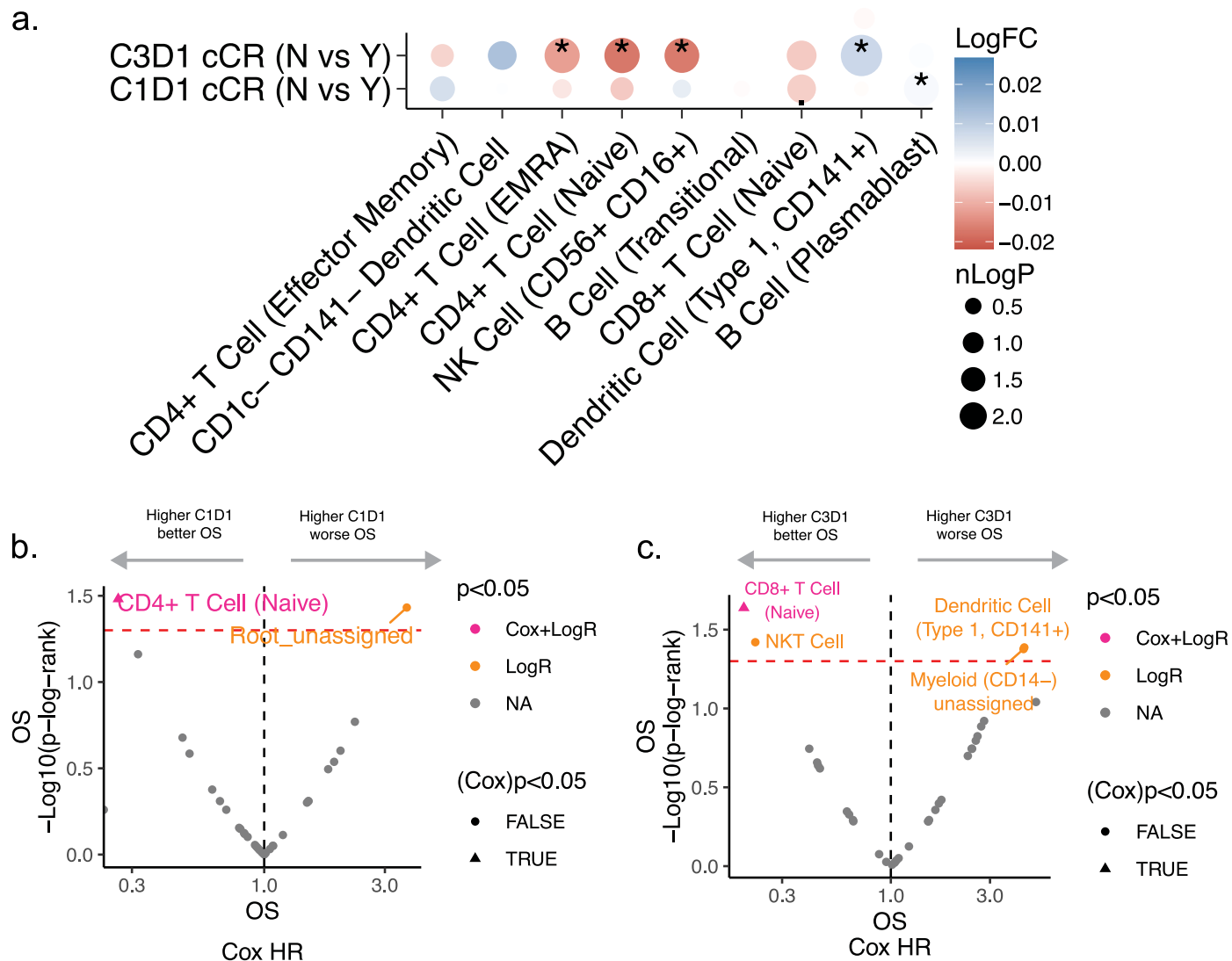
wall mass and post- gemcitabine, cisplatin, plus nivolumab MRI sequences scored as VI-RADS 5. **(c)** Distribution of VI-RADS scores on MRI of the bladder post- gemcitabine, cisplatin, plus nivolumab (n = 50). **(d)** Landmark analysis for metastasis-free survival in study cohort with available restaging MRI scans (n = 50) according to VI-RADS 1-2 versus 3–5.





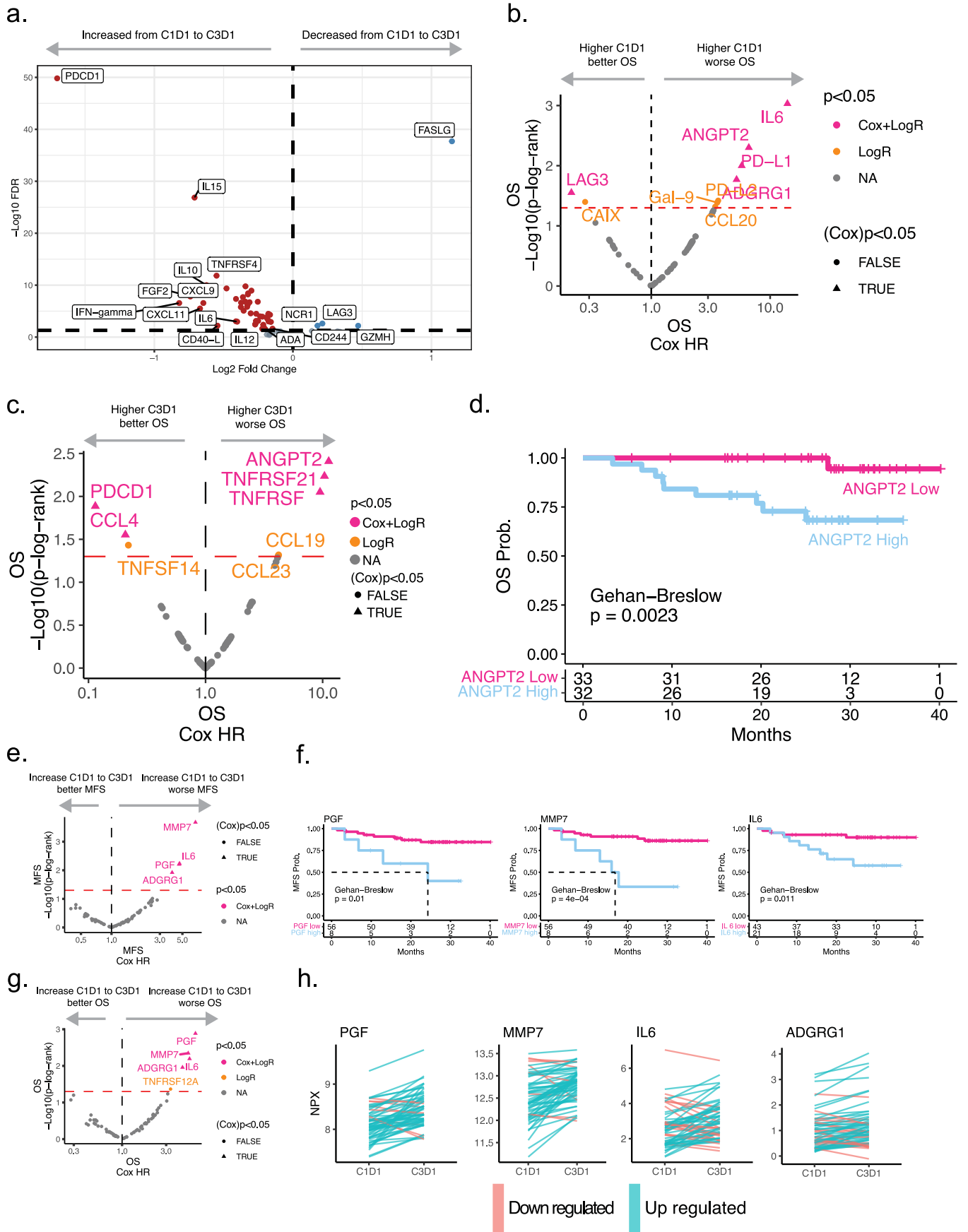
**Extended Data Fig. 3 | Relationship between PD-L1 immunohistochemical staining of pre-treatment transurethral resection of bladder tumor specimens (n = 59) and clinical outcomes. (a)** Relationship between PD-L1 immunohistochemical staining and scoring according to the combined positive score (CPS) and achievement of a clinical complete response (Y, yes; N, no) in 59 patients with available samples for testing. Box and whisker plots demonstrating CPS for patients achieving a clinical complete response (min 0, max 95, median

5, 1<sup>st</sup> quartile 1, 3<sup>rd</sup> quartile 20) and not achieving a clinical complete response (min 0, max 95, median 1, 1<sup>st</sup> quartile 0, 3<sup>rd</sup> quartile 5). **(b)** Kaplan–Meier curve for metastasis-free survival according to PD-L1 expression of baseline TURBT specimens using the cut-point of CPS ≥10 versus <10. **(c)** Kaplan–Meier curve for overall survival according to PD-L1 expression of baseline TURBT specimens using the cut-point of CPS ≥10 versus <10.



**Extended Data Fig. 4 | Peripheral blood mass cytometry (CyTOF) and association with response and overall survival.** (a) Heatmap, showing the differential abundance results between cell populations and association with clinical complete response (cCR). The x-axis shows the cell type annotation from ASTROLABE. The y-axis shows the timepoint of the comparison between responders (Y) and non-responders (N). The direction of the logFC is dictated by the comparison. Negative logFC indicates increase of expression in responders. The size of the circle indicates the significance. The larger the circle the smaller the p value. Additionally, the stars on top of the circles indicate  $p < 0.05$  significance. Circles without stars indicate  $p > 0.05$  or non-statistically

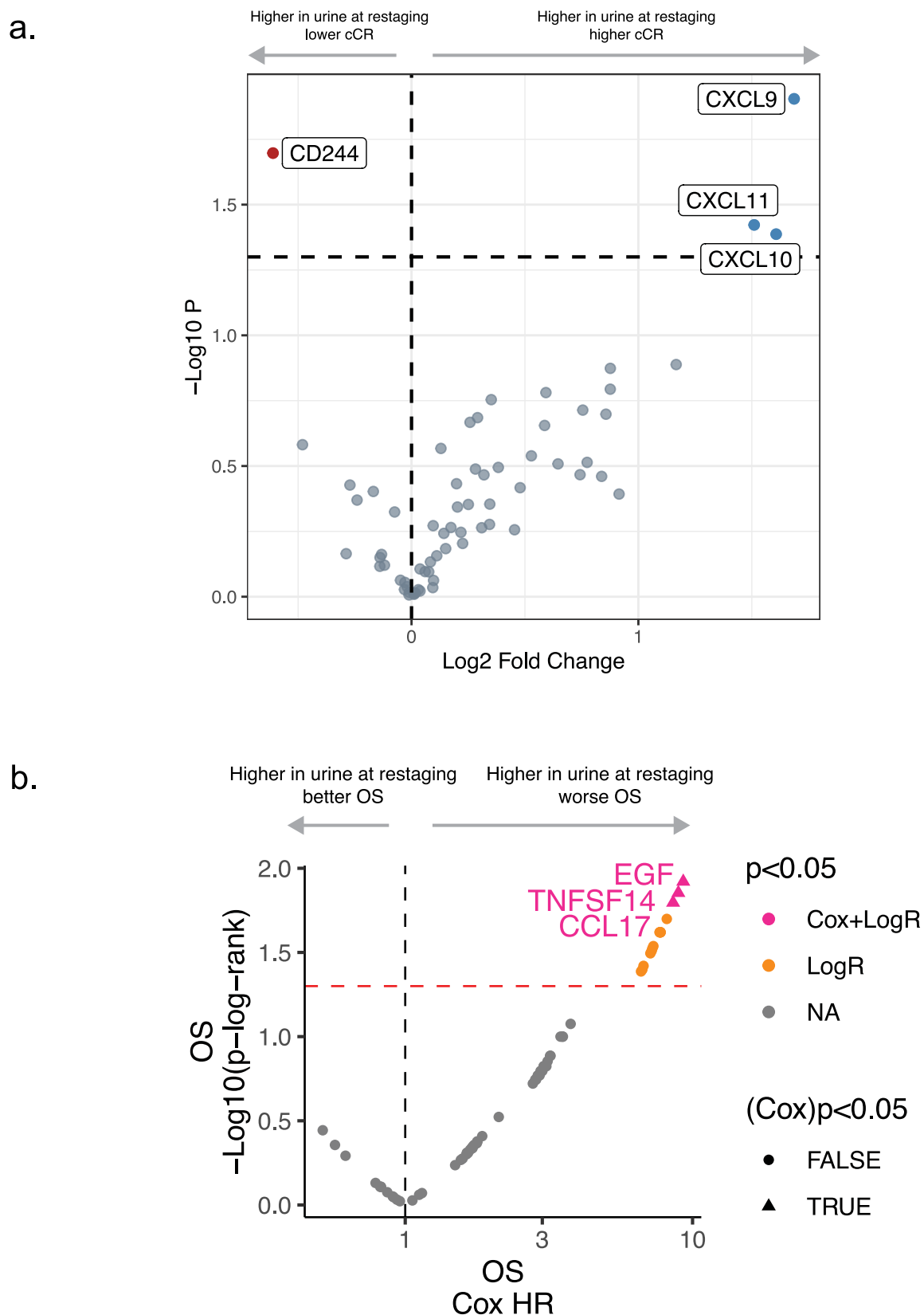
significant. (b) Peripheral blood CyTOF data. Volcano plot for overall survival (OS) based on cycle 1 day 1 (C1D1) abundances of cell populations showing log rank test (y-axis) and Cox regression hazard ratio (x-axis). Cell abundances significant for both tests are shown in pink. A lower hazard ratio (left side of the black line) is associated with reduced risk. (c) Peripheral blood CyTOF data. Volcano plot for OS based on cycle 3 day 1 (C3D1) abundances of cell populations showing log rank test (y-axis) and Cox regression hazard ratio (x-axis). Cell abundances significant for both tests are shown in pink. A lower hazard ratio (left side of the black line) is associated with reduced risk.



Extended Data Fig. 5 | See next page for caption.

**Extended Data Fig. 5 | Peripheral blood protein analytes and association with response and overall survival.** (a) Volcano plot demonstrating trend in peripheral blood analytes by Olink from cycle 1 day 1 (C1D1) to cycle 3 day 1 (C3D1) demonstrating largest increase in PD-1 (PDCD1). (b) Peripheral blood protein analyte data. Volcano plot for overall survival (OS) based on C1D1 levels of protein analytes showing log rank test (y-axis) and Cox regression hazard ratio (x-axis). Analytes significant for both tests are shown in pink. A lower hazard ratio (left side of the black line) is associated with reduced risk. (c) Peripheral blood protein analyte data. Volcano plot for overall survival (OS) based on C3D1 levels of protein analytes showing log rank test (y-axis) and Cox regression hazard ratio (x-axis). Analytes significant for both tests are shown in pink. A lower hazard ratio (left side of the black line) is associated with reduced risk. (d) Kaplan-Meier curves showing better OS as measured from C3D1 in patients with lower versus higher peripheral blood levels of angiopoietin-2 (ANGPT2). (e) Peripheral blood protein

analyte data. Volcano plot for metastasis-free survival (MFS) based on changes in levels of protein analytes from C1D1 to C3D1 showing log rank test (y-axis) and Cox regression hazard ratio (x-axis). Analytes significant for both tests are shown in pink. A lower hazard ratio (left side of the black line) is associated with reduced risk. (f) Kaplan-Meier curves for the proteins in E showing MFS for patients with an increase in PGF, MMP7, or IL6 from C1D1 to C3D1 versus a decrease in levels of these proteins. (g) Peripheral blood protein analyte data. Volcano plot for OS based on changes in levels of protein analytes from C1D1 to C3D1 showing log rank test (y-axis) and Cox regression hazard ratio (x-axis). Analytes significant for both tests are shown in pink. A lower hazard ratio (left side of the black line) is associated with reduced risk. (h) Peripheral blood protein analyte data. Line plots showing individual changes in protein levels from C1D1 to C3D1. N = 64 patients for each analyte for C1D1 to C3D1 comparisons.



**Extended Data Fig. 6 | Urine protein analytes and association with response and survival.** (a) Urine Olink protein analyte data. Volcano plot showing the differential expression at time of restaging among patients achieving or not achieving a clinical complete response. The statistical significance or  $-\log_{10}(P\text{val})$  is shown on y-axis and  $\log_2$  protein levels is shown on x-axis.

(b) Urine protein analyte data. Volcano plot for overall survival (OS) based levels of protein analytes in the urine at the time of restaging showing log rank test (y-axis) and Cox regression hazard ratio (x-axis). Analytes significant for both tests are shown in pink. A lower hazard ratio (left side of the black line) is associated with reduced risk.

Extended Data Table 1 | Association between baseline clinical stage and cCR rate

<b>Baseline T stage</b>	<b>Clinical Complete Response Rate</b>	<b>P-value (Fisher's exact test)</b>
cT2	24/43 (56%; 95% CI: 40%, 71%)	0.04
cT3	6/24 (25%; 95% CI: 10%, 47%)	
cT4	3/9 (33%; 95% CI: 8%, 70%)	

Extended Data Table 2 | Number of treatment-emergent grade  $\geq 3$  adverse events occurring in  $\geq 10\%$  patient(s)\* (n=76 patients) per NCI CTCAE version 4.03

Adverse Event	Grade 1	Grade 2	Grade 3	Grade 4
Fatigue	46	12	0	0
Anemia	22	23	12	0
Neutrophil count decreased	7	19	21	5
Nausea	39	5	0	0
Constipation	38	1	0	0
Creatinine increased	23	15	0	0
Hypertension	19	13	4	0
Hyperglycemia	27	5	2	0
White blood cell decreased	17	11	3	0
Platelet count decreased	21	5	2	2
Hematuria	25	1	3	0
Anorexia	18	5	0	0
Hyponatremia	17	1	4	1
Tinnitus	22	1	0	0
Dyspnea	19	2	1	0
Alopecia	21	0	0	0
Urinary tract infection	3	5	13	0
Back pain	15	2	0	0
Insomnia	13	2	0	0
Urinary frequency	14	1	0	0
Hypomagnesemia	7	7	0	0
Vomiting	12	1	1	0
Abdominal pain	7	4	2	0
Rash maculo-papular	11	2	0	0
Diarrhea	11	1	0	0
Hypoalbuminemia	9	3	0	0
Hypokalemia	9	0	3	0
Pain	10	1	1	0
Proteinuria	5	7	0	0
Urinary tract pain	10	2	0	0
Headache	10	1	0	0
Hypocalcemia	9	2	0	0
Pruritus	10	1	0	0
Skin and subcutaneous tissue disorders	9	2	0	0
Weight loss	5	6	0	0
Alanine aminotransferase increased	8	2	0	0
Anxiety	6	2	1	0
Aspartate aminotransferase increased	7	1	1	0
Dizziness	8	1	0	0
Dysgeusia	8	1	0	0
Peripheral sensory neuropathy	9	0	0	0
Urinary urgency	9	0	0	0
Cough	8	0	0	0
Depression	5	1	1	1
Edema limbs	8	0	0	0
Hyperkalemia	7	1	0	0

\*maximum grade event for each term per patient

**Extended Data Table 3 | Association between pre-specified genomic alterations in pre-treatment transurethral resection of bladder tumor tissue and likelihood of achieving a cCR. P values are based on Fisher's exact test**

Genomic Alternation*		cCR	No cCR	OR (95% CI)	P value	BH FDRs	Adjusted p values
<i>ATM</i> *	Mutant	6	8	0.90 (0.26, 3.01)	1.0000	1.0000	1.0000
	Wild type	25	30				
<i>FANCC</i> *	Mutant	1	0		0.4493	0.6490	0.6490
	Wild type	30	38				
<i>RB1</i> *	Mutant	6	11	0.59 (0.18, 1.85)	0.4107	0.6674	0.6490
	Wild type	25	27				
<i>RB1</i> (pathogenic)*	Mutant	5	10	0.54 (0.15, 1.80)	0.3858	1.0000	0.6490
	Wild type	26	28				
<i>ERCC2</i> *	Mutant	5	2	3.46 (0.62, 26.99)	0.2301	0.9971	0.6490
	Wild type	26	36				
<i>ERCC2</i> (pathogenic)*	Mutant	4	2	2.67 (0.43, 21.81)	0.3974	0.7380	0.6490
	Wild type	27	36				
FANCC, ATM, and/or RB1 (any)*	Mutant	12	17	0.78 (0.29, 2.07)	0.6337	0.8238	0.8238
	Wild type	19	21				
FANCC, ATM, and/or RB1 (pathogenic)*	Mutant	5	10	0.54 (0.15, 1.80)	0.3858	0.8359	0.6490
	Wild type	26	28				
FANCC, ATM, RB1, and/or ERCC2 (any)*	Mutant	15	18	1.04 (0.40, 2.73)	1.0000	1.0000	1.0000
	Wild type	16	20				
FANCC, ATM, RB1, and/or ERCC2 (pathogenic)*	Mutant	8	11	0.85 (0.28, 2.52)	0.7940	0.9384	0.9384
	Wild type	23	27				
TMB†	TMB ≥ 10 mut/Mb	21	15	3.42 (1.22, 9.71)	0.0261	0.3393	0.3393
	TMB <10 mut/Mb	9	22				
FANCC, ATM, RB1, ERCC2 (any), and/or high TMB*	Mutant	23	23	1.88 (0.66, 5.47)	0.3066	0.9964	0.6490
	Wild type	8	15				
FANCC, ATM, RB1, ERCC2 (pathogenic), and/or high TMB*	Mutant	22	19	2.44 (0.89, 6.84)	0.0904	0.5876	0.5876
	Wild type	9	19				

TMB, tumor mutational burden; BH FDRs, Benjamini-Hochberg False Discovery Rate

\*Analyses of genomic alterations in *ATM*, *FANCC*, and *RB1* include n=69 (of 76 total study patients) for each matrix. Seven patients excluded from the analysis for the following reasons: 3 patients for whom no DNA sequencing is available and 4 patients who did not undergo clinical response assessment.

†Analysis of TMB includes n=67 (of 76 total study patients). Nine patients excluded from the analysis for the following reasons: 5 patients for whom no DNA sequencing is available and/or no TMB value could be calculated and 4 patients who did not undergo clinical response assessment.



## Reporting Summary

Nature Portfolio wishes to improve the reproducibility of the work that we publish. This form provides structure for consistency and transparency in reporting. For further information on Nature Portfolio policies, see our [Editorial Policies](#) and the [Editorial Policy Checklist](#).

### Statistics

For all statistical analyses, confirm that the following items are present in the figure legend, table legend, main text, or Methods section.

- | n/a                                 | Confirmed  |
|-------------------------------------|--|
| <input type="checkbox"/>            | <input checked="" type="checkbox"/> The exact sample size ( $n$ ) for each experimental group/condition, given as a discrete number and unit of measurement  |
| <input checked="" type="checkbox"/> | <input type="checkbox"/> A statement on whether measurements were taken from distinct samples or whether the same sample was measured repeatedly   |
| <input type="checkbox"/>            | <input checked="" type="checkbox"/> The statistical test(s) used AND whether they are one- or two-sided<br><i>Only common tests should be described solely by name; describe more complex techniques in the Methods section.</i>   |
| <input type="checkbox"/>            | <input checked="" type="checkbox"/> A description of all covariates tested   |
| <input type="checkbox"/>            | <input checked="" type="checkbox"/> A description of any assumptions or corrections, such as tests of normality and adjustment for multiple comparisons  |
| <input type="checkbox"/>            | <input checked="" type="checkbox"/> A full description of the statistical parameters including central tendency (e.g. means) or other basic estimates (e.g. regression coefficient) AND variation (e.g. standard deviation) or associated estimates of uncertainty (e.g. confidence intervals) |
| <input type="checkbox"/>            | <input checked="" type="checkbox"/> For null hypothesis testing, the test statistic (e.g. $F$ , $t$ , $r$ ) with confidence intervals, effect sizes, degrees of freedom and $P$ value noted<br><i>Give <math>P</math> values as exact values whenever suitable.</i>                            |
| <input checked="" type="checkbox"/> | <input type="checkbox"/> For Bayesian analysis, information on the choice of priors and Markov chain Monte Carlo settings  |
| <input checked="" type="checkbox"/> | <input type="checkbox"/> For hierarchical and complex designs, identification of the appropriate level for tests and full reporting of outcomes  |
| <input checked="" type="checkbox"/> | <input type="checkbox"/> Estimates of effect sizes (e.g. Cohen's $d$ , Pearson's $r$ ), indicating how they were calculated  |

*Our web collection on [statistics for biologists](#) contains articles on many of the points above.*

### Software and code

Policy information about [availability of computer code](#)

Data collection

Data analysis

For manuscripts utilizing custom algorithms or software that are central to the research but not yet described in published literature, software must be made available to editors and reviewers. We strongly encourage code deposition in a community repository (e.g. GitHub). See the Nature Portfolio [guidelines for submitting code & software](#) for further information.

### Data

Policy information about [availability of data](#)

All manuscripts must include a [data availability statement](#). This statement should provide the following information, where applicable:

- Accession codes, unique identifiers, or web links for publicly available datasets
- A description of any restrictions on data availability
- For clinical datasets or third party data, please ensure that the statement adheres to our [policy](#)

In accordance with NIH's Genomic Data Sharing Policy, the DNA sequencing data used to support the findings of this study has been deposited under controlled-access in the database of Genotypes and Phenotypes (dbGaP) under the accession number phs0003372. Genomic, clinical, mass cytometry, and protein analyte data from this study used to support this publication will be made available upon reasonable request from a qualified medical or scientific professional for the

specific purpose laid out in that request and may include de-identified individual participant data. Requests for secondary use of this data will require completing a data use agreement ([https://osp.od.nih.gov/wp-content/uploads/Model\\_DUC.pdf](https://osp.od.nih.gov/wp-content/uploads/Model_DUC.pdf)) and submitting a data access request to NIH.

## Human research participants

Policy information about [studies involving human research participants and Sex and Gender in Research](#).

Reporting on sex and gender	Our study reports a phase 2 trial in patients with muscle-invasive bladder cancer. Men are approximately 4 times more likely to be diagnosed with bladder cancer. Our study enrolled 79% men and 21% women.
Population characteristics	The baseline characteristics are outlined in Table 1 of the manuscript and are consistent with the demographics of muscle-invasive bladder cancer in the United States.
Recruitment	Patients were recruited from urology and medical oncology clinics at participating institutions. Patients were recruited from those seeking standard evaluation and clinical care for muscle-invasive bladder cancer in these clinics and all patients seen for routine clinical care were offered the option of trial participation if deemed potentially eligible.
Ethics oversight	The protocol was approved by local ethics committees at the Icahn School of Medicine at Mount Sinai, City of Hope Comprehensive Cancer Centers, Huntsman Cancer Institute University of Utah, Oregon Health and Science University, Penn Medicine Abramson Cancer Center, Rutgers Cancer Institute of New Jersey, University of Southern California, and University of Wisconsin and written informed consent was provided by all patients prior to enrollment.

Note that full information on the approval of the study protocol must also be provided in the manuscript.

## Field-specific reporting

Please select the one below that is the best fit for your research. If you are not sure, read the appropriate sections before making your selection.

Life sciences  Behavioural & social sciences  Ecological, evolutionary & environmental sciences

For a reference copy of the document with all sections, see [nature.com/documents/nr-reporting-summary-flat.pdf](https://nature.com/documents/nr-reporting-summary-flat.pdf)

## Life sciences study design

All studies must disclose on these points even when the disclosure is negative.

Sample size	The co-primary objectives of the study were to: (a) determine the cCR rate with gemcitabine, cisplatin, plus nivolumab and (b) determine the ability of cCR to predict clinical benefit from treatment. Clinical benefit was defined as either: (a) being metastasis-free at 2 years in patients achieving a cCR and opting to not undergo immediate cystectomy or (b) achieving a pCR (<pT1) in patients with a cCR opting for immediate cystectomy. Secondary objectives included the association between genomic alterations in a prespecified panel of genes detected in pre-treatment TURBT tissue (ERCC2, ATM, RB1, and FANCC 15–22), as well as tumor mutational burden (using an established cut-point of $\geq 10$ mutations/Mb <sup>23,24</sup> ), and clinical outcomes. Additional secondary objectives included safety, metastasis-free survival, overall survival, and bladder-intact survival. The sample size was based on the following assumptions: (a) patients without a cCR would not be suitable to forgo cystectomy, (b) ~40% of enrolled patients would achieve a cCR, and (c) ~35% of enrolled patients would achieve clinical benefit. Therefore, our assumption implied that the negative predictive value of a cCR would be 1. The sample size was based on the confidence interval width of the positive predictive value of cCR for clinical benefit and generated such that the lower bound of the 95% one-sided confidence interval exceeded 80%. This required enrollment of 68 patients and the sample size was increased to 76 to account for potential missing data.
Data exclusions	No data were excluded from the analysis.
Replication	This was a prospective clinical trial and replication was not within the scope of the trial.
Randomization	This was a phase 2 single arm trial employing a risk-adapted strategy and randomization was not deemed appropriate to the design prior to conducting this phase 2 portion which could then be used to inform the design of a randomized trial.
Blinding	There was no randomization in this trial and therefore blinding was not applicable.

## Reporting for specific materials, systems and methods

We require information from authors about some types of materials, experimental systems and methods used in many studies. Here, indicate whether each material, system or method listed is relevant to your study. If you are not sure if a list item applies to your research, read the appropriate section before selecting a response.

## Materials &amp; experimental systems

## Methods

n/a	Involved in the study
<input type="checkbox"/>	<input checked="" type="checkbox"/> Antibodies
<input checked="" type="checkbox"/>	<input type="checkbox"/> Eukaryotic cell lines
<input checked="" type="checkbox"/>	<input type="checkbox"/> Palaeontology and archaeology
<input checked="" type="checkbox"/>	<input type="checkbox"/> Animals and other organisms
<input type="checkbox"/>	<input checked="" type="checkbox"/> Clinical data
<input checked="" type="checkbox"/>	<input type="checkbox"/> Dual use research of concern

n/a	Involved in the study
<input checked="" type="checkbox"/>	<input type="checkbox"/> ChIP-seq
<input checked="" type="checkbox"/>	<input type="checkbox"/> Flow cytometry
<input checked="" type="checkbox"/>	<input type="checkbox"/> MRI-based neuroimaging

## Antibodies

## Antibodies used

Channel Target Clone Manufacturer Catalog #  
 89Y CD45 HI30 Standard Bio Tools 3089003B  
 113In CD57 HNK-1 Biologend 359602  
 115In CD11c BU15 Biologend 337202  
 141Pr CD33 WM53 Biologend 303410  
 142Nd CD19 REA675 Miltenyi 130-122-301  
 143Nd CD45RA REA562 Miltenyi 130-122-292  
 144Nd CD141 Phx-01 Biologend 902101  
 145Nd CD4 REA623 Miltenyi 130-122-283  
 146Nd CD8 REA734 Miltenyi 130-122-281  
 147Sm CLEC9A 8F9 Miltenyi 130-122-306  
 148Nd CD16 REA423 Miltenyi 130-108-027  
 149Sm CD127 A019D5 Standard Bio Tools 3149011B  
 150Nd CD1c REA694 Miltenyi 130-122-298  
 151Eu CD123 REA918 Miltenyi 130-122-297  
 152Sm CD66b REA306 Miltenyi 130-108-019  
 154Sm ICOS C398.4A Biologend 313502  
 155Gd CD27 REA499 Miltenyi 130-122-295  
 156Gd PD-L1 29E.2A3 Biologend 329710  
 158Gd CD103 Ber-ACT8 BioLegend 350202  
 159Tb CD24 ML5 Biologend 311102  
 160Gd CD14 REA599 Miltenyi 130-122-290  
 161Dy CD56 REA196 Miltenyi 130-108-016  
 162Dy gdTCR REA591 Miltenyi 130-122-291  
 163Dy CXCR5 REA103 Miltenyi 130-122-325  
 164Dy CD69 FN50 Biologend 310939  
 165Ho CD64 10.1 Biologend 305016  
 166Er 41BB 4B4-1 Biologend 309802  
 167Er CCR7 REA546 Miltenyi 130-122-300  
 168Er CD3 REA613 Miltenyi 130-122-282  
 169Tm CD25 REA570 Miltenyi 130-122-302  
 170Er CD38 REA671 Miltenyi 130-122-288  
 171Yb CD161 HP-3G10 BioLegend 339902  
 172Yb CD39 A1 Biologend 328202  
 173Yb CXCR3 REA232 Miltenyi 130-108-022  
 174Yb HLADR REA805 Miltenyi 130-122-299  
 175Lu PD-1 EH12.2H7 Standard Bio Tools 3174020B  
 176Yb CCR4 REA279 Miltenyi 130-122-323  
 209Bi CD11b ICRF44 Standard Bio Tools 3209003B

## Validation

All antibodies were either purchased pre-conjugated from Fluidigm (Fluidigm, South San Francisco, CA) or conjugated in-house (using commercial X8 polymer conjugation kits purchased from Fluidigm) at the Human Immune Monitoring Center (HIMC), Icahn School of Medicine at Mount Sinai, New York. All in-house conjugated antibodies were titrated and validated on healthy donor PBMCs.

## Clinical data

Policy information about [clinical studies](#)

All manuscripts should comply with the ICMJE [guidelines for publication of clinical research](#) and a completed [CONSORT checklist](#) must be included with all submissions.

Clinical trial registration

Study protocol

Data collection

Our primary goal was to test whether uniformly assessed and consistently defined cCR could identify patients who could safely forgo immediate cystectomy. We reasoned that a potentially effective personalized risk-adapted strategy would: (a) tolerate missing some patients who might have been suitable candidates to forgo immediate cystectomy in favor of maximizing identification of patients who fare well without immediate cystectomy and (b) incorporate the ability of later cystectomy to achieve favorable cancer-related outcomes in the subset of patients with a cCR experiencing local recurrence after initial surveillance. Therefore, our primary objectives were to estimate the cCR rate and to assess the positive predictive value of cCR for a composite outcome measure (2-year metastasis-free survival in patients forgoing immediate cystectomy or <ypT1N0 in patients electing immediate cystectomy). Secondary outcomes included safety, the association between a prespecified panel of genomic biomarkers and clinical complete response and metastasis free survival, metastasis free survival, and overall survival. These outcomes were predefined at the time of designing the study as were used to inform the clinical trial protocol.